



# Experimental investigation of the temperature coefficients of $V_{mpp}$ and $I_{mpp}$ in a silicon solar cell

By  
Sjur Narten Christiansen

SUPERVISORS  
Rune Strandberg  
Sissel Tind Kristensen

University of Agder, 2019  
Faculty of Engineering and Science  
Department of Engineering Sciences



## Abstract

This thesis is meant to provide an experimental investigation of the temperature coefficient ( $\beta$ ) of  $V_{mpp}$  compared to  $V_{oc}$  in a multicrystalline silicon solar cell. With the main question being: to what degree is the temperature coefficient equal for  $V_{oc}$  and  $V_{mpp}$  and how does series losses ( $R_s$ ) affect the two? Also investigating the same question for  $I_{sc}$  and  $I_{mpp}$ . Three types of multicrystalline cells have been measured using a NeonSee AAA sun simulator, for a total of 18 tested cells all produced by Elkem Solar Silicon. I-V data was collected using temperature scan, Suns-Voc and Isc-Voc measurements, with temperatures reflecting normal operation range for solar cells, from 25 to 65°C. The different cells tested have been Al-BSF, PERC 0.5 and PERC 1.3 cells. The resulting data has been calculated using Excel providing  $\beta$  results for  $V_{oc}$ ,  $V_{mpp}$ ,  $I_{sc}$  and  $I_{mpp}$ . For all  $\beta$  results, standard deviation of slope was also calculated to say something about the accuracy of the measurements.

Results from the analysed data show a trend where  $\beta_{V_{oc}}$  is statistically significant different from  $\beta_{V_{mpp}}$ . This is concluded based on the results where the majority cells tested show  $\beta_{V_{oc}}$  having a larger value than  $\beta_{V_{mpp}}$ , without any overlapping in standard deviation. The degree of difference varies with the different cells and the different measuring techniques. As for the effect of  $R_s$ , the difference in results between the Tscan measuring technique and the Suns-Voc and Isc-Voc techniques have been analysed. A trend of lower values for  $\beta_{V_{mpp}}$  from Tscan measurements indicates that  $R_s$  has a negative effect on the  $\beta_{V_{mpp}}$ . Generally, the results show that  $\beta$  for current is more varying than for voltage data. Results compared between the different measuring techniques are showing less visible trends for  $\beta_{I_{sc}}$  and  $\beta_{I_{mpp}}$  than for  $\beta_{V_{oc}}$  and  $\beta_{V_{mpp}}$ . There are less systematic differences between Tscan data and the two other methods. This is probably because  $R_s$  should have little or no effect on the current.


For most of the cells calculated, standard deviation is very low for both current and voltage calculations, which is a sign that the measurements are accurate, however more testing is required to state more conclusive evidence.

## Acknowledgements

I would like to sincerely thank PhD. Research Fello, Sissel Tind Kristensen for all her excellent guidance in the PV lab and for sharing her knowledge and enthusiasm for the solar energy field. Sissel has also been available with an open office door and on email to answer any question the entirety of the duration of this work.

I would also like to thank Rune Standberg for counselling and theoretical input to help find the right way to work the lab data and to always provide new angles on problems.

University of Agder, Grimstad



---

Sjur Narten Christiansen

January 11th 2019

## Individual Mandatory Declaration

1.	I/We hereby declare that my/our thesis is my/our own work and that I/We have not used any other sources or have received any other help than mentioned in the thesis.	<input checked="" type="checkbox"/>
2.	I/we further declare that this thesis: <ul style="list-style-type: none"> <li>- has not been used for another exam at another department/university/university college in Norway or abroad;</li> <li>- does not refer to the work of others without it being stated;</li> <li>- does not refer to own previous work without it being stated;</li> <li>- have all the references given in the literature list;</li> <li>- is not a copy, duplicate or copy of another's work or manuscript.</li> </ul>	<input checked="" type="checkbox"/>
3.	I/we am/are aware that violation of the above is regarded as cheating and may result in cancellation of exams and exclusion from universities and colleges in Norway, see Universitets- og høyskoleloven §§4-7 og 4-8 og Forskrift om eksamen §§ 31.	<input checked="" type="checkbox"/>
4.	I/we am/are aware that all submitted theses may be checked for plagiarism.	<input checked="" type="checkbox"/>
5.	I/we am/are aware that the University of Agder will deal with all cases where there is suspicion of cheating according to the university's guidelines for dealing with cases of cheating.	<input checked="" type="checkbox"/>
6.	I/we have incorporated the rules and guidelines in the use of sources and references on the library's web pages.	<input checked="" type="checkbox"/>

### Publishing Agreement

Authorization for electronic publishing of the thesis.

Author(s) have copyrights of the thesis. This means, among other things, the exclusive right to make the work available to the general public (Åndsverkloven. §2).

All theses that fulfill the criteria will be registered and published in Brage Aura and on UiA's web pages with author's approval.

Theses that are not public or are confidential will not be published.

I hereby give the University of Agder a free right to make the task available for electronic publishing:

YES  NO

Is the thesis confidential?

YES  NO

(confidential agreement must be completed)

- If yes:

Can the thesis be published when the confidentiality period is over?  YES  NO

Is the task except for public disclosure?

YES  NO

(contains confidential information. see Offl. §13/Fvl. §13)

## Table of Contents

<b>Chapter 1: Introduction .....</b>	<b>1</b>
1.1 Thesis objectives .....	2
1.2 Research questions .....	2
<b>Chapter 2: Theory .....</b>	<b>3</b>
2.1 Solar radiation.....	3
2.2 Photovoltaic cells .....	4
2.2.1 Cell material and Construction .....	4
2.3 The IV curve .....	7
2.4 Effect of temperature in silicon solar cells.....	9
2.5 Production of silicon solar cells.....	10
2.5.1 Silicon production .....	10
2.5.2 Cell production .....	11
<b>Chapter 3: Method .....</b>	<b>12</b>
3.1 Light soaking.....	12
3.2 Measurements .....	13
3.2.1 Calibration .....	13
3.2.2 Accuracy .....	14
3.2.3 Temperature scan .....	14
3.2.4 Suns -Voc and Isc – Voc.....	14
3.2.5 Lab time and routines.....	15
3.2.6 Cells tested.....	15
3.3 Data analysis .....	17
3.3.1 Comparison between IV curve measurements.....	17
3.3.2 Temperature coefficients .....	18
3.3.3 Plotting temperature coefficients using LINEST.....	19
<b>Chapter 4: Results and discussion .....</b>	<b>20</b>
4.1 Voc and Vmpp temperature coefficient.....	20
4.1.1 Al-BSF cells .....	21
4.1.2 PERC 0.5 cells .....	22
4.1.3 PERC 1.3 cells .....	23
4.2 Discussion for Voc and Vmpp measurements .....	24

4.3	Isc and Impp temperature coefficient.....	26
4.3.1	Al-BFS cells .....	26
4.3.2	PERC 0.5 cells .....	27
4.3.3	PERC 1.3 cells .....	28
4.4	Discussion for Isc and Impp .....	29
<b>Chapter 5: Conclusion .....</b>		<b>30</b>
5.1	Future Work.....	31
<b>Chapter 6: List of References .....</b>		<b>32</b>
<b>Chapter 7: Appendix .....</b>		<b>34</b>
7.1	Appendix A.....	34
7.2	Appendix B.....	37

## List of Figures

Figure 1-1	Spectrum of solar radiation [12].....	3
Figur 2-1	Schematic representation of covalent bonds in a silicon crystal lattice. [13] .....	4
Figur 2-2	Illustration of band gap in semiconductor and a p-n junction[16, 17].....	5
Figur 2-3	Simplified cross section view of a silicon solar cell.[18].....	6
Figur 2-4	Typical IV curve of a PV cell [19] .....	7
Figur 2-5	IV curve with performance impairments[19] .....	8
Figur 2-6	Correlation between cell parameters and temperature .....	9
Figur 2-7	Temperature coefficients of different Photovoltaic devices[9].....	10
Figur 2-8	Mono- and multi-crystalline PV cells [23].....	11
Figur 3-1	Light soaking rig at the UiA PV lab .....	12
Figur 3-2	Sun simulator : NeonSee BIV-HCSS-21 [27].....	13
Figur 3-3	Voc and Vmpp in STC for each cell for A-BSF, PERC 0.5 and PERC 1.3.....	16
Figur 3-4	Isc-Voc, Suns-Voc and Tscan, IV comparison for 2099-07-005.....	17
Figur 3-5	Suns-Voc measured Voltage per temperature for cell 3645-22-022.....	18
Figur 4-1	(a) and (b) Al-BSF $\beta$ for Voc and Vmpp .....	21
Figur 4-2	(a) and (b) PERC 0.5 $\beta$ for Voc and Vmpp .....	22
Figur 4-3	(a) and (b) PERC 1.3 $\beta$ for Voc and Vmpp .....	23
Figur 4-4	(a) and (b) Al-BSF $\beta$ for Isc and Impp .....	26
Figur 4-5	(a) and (b) PERC 0.5 $\beta$ for Isc and Impp .....	27
Figur 4-6	(a) and (b) PERC 1.3 $\beta$ for Isc and Impp .....	28

## Abbreviations

PV	Photovoltaic
Wh	Watt hour
kWh	Kilo watt hour
Si	Silicon
c-Si	Crystalline Silicon
mono-Si	Monocrystalline Silicon
mc-Si	Multicrystalline Silicon
V	Voltage
Voc	Open circuit voltage
V <sub>mpp</sub>	Maximum power point voltage
I	Current
I <sub>sc</sub>	Short circuit current
I <sub>mpp</sub>	Maximum power point current
FF	Fill factor
P	Power
P <sub>mpp</sub>	Maximum Power
R <sub>s</sub>	Series losses
$\beta$	Temperature coefficient
LID	Light induced degradation
Al-BSF	Aluminium-back surface field
PERC	Passivated emitter and rear cell



## Chapter 1: Introduction

The energy from the sun is the biggest and most important energy source in the world. Still, most of the energy used today is old solar energy that has been stored underground for thousands of years. Fissile fuels have been the most important energy source in modern history[1]. Even though we have adapted to a life where we rely on these ancient sources of energy, it does not mean it has to stay this way. One common estimate is that the accumulated solar energy that reaches the surface of the earth every year is 15,000 times bigger than the yearly energy consumption[2]. Renewable energy has seen rapid growth the past decade and today photovoltaic (PV) power is leading the way. PV has the last years seen an accelerating growth, over the course of 2016 the total installed PV capacity rose with about 33% which is at least 98 GW. And the rise has continued making the total worldwide installed PV capacity at approximately 402 GW by the end of 2017 [3]. Together renewable energy stood for 24% of global electricity production in 2017 [4].

Electricity is the most universal energy carrier today and the use of PV systems is now the best way to transform solar energy directly into electric energy. The efficiency of PV cells is continuing to rise, as technology is evolving rapidly in the renewable field due to increased awareness and focus on improvement. The most used material in converting solar radiation to electricity today is crystalline silicon (c-Si), with 95% of the worldwide PV production[5]. The c-Si cell is a stable and well tested technology which has proven to be effective for electricity production, with record efficiencies of lab cells at 26.7% for mono-crystalline cells and 22.3 for multi-crystalline cells in 2017[6]. In commercial use the efficiency numbers are lower, however in the past decade wafer based silicon modules have increased from about 12% to 17% efficiency (with some producing as high as 21%)2017[7]. PV technology will never be able to reach 100% efficiency with current methods due to limiting factors, mainly thermalization and transmission losses[8]. However, there is still plenty of room for improvement in existing PV technology. Currently several aspects of the PV technology are being researched to improve performance and lower material, which together effectively lowers the prices[4].

It is well known that PV devices are naturally dependent of temperature and different operating temperatures affect the performance of the device[9]. With the evolution of PV technology there has been an expanding interest for theory and experience research of how temperature affects the main parameters of a PV device. For most PV devices an increase in temperature means a decrease in power[10]. The effects of temperature are widely known, and the temperature dependency of a device is in some way considered when planning a PV installation. Temperature coefficient ( $\beta$ ) is a way to quantify how much a parameter change per degree of temperature change,  $\beta$  will be further explained in chapter 2. There is still room for expanding the knowledge effects the  $\beta$  of individual parameters in PV devices. Deeper understanding the temperature in PV devices may prove important to improvement in PV technology[8].

## 1.1 Thesis objectives

The parameters mentioned in this section will be explained in Chapter 2.

In this thesis an experimental investigation of the  $\beta$  of the voltage and current parameters for a selection of multicrystalline solar cells that vary in cell architecture, resistivity and position in the silicon ingot. More specifically the  $\beta$  of the open circuit voltage ( $V_{oc}$ ) will be compared to the  $\beta$  of the maximum power point voltage ( $V_{mpp}$ ). The same will be done for the  $\beta$  of the short circuit current ( $I_{sc}$ ) and the maximum power point current ( $I_{mpp}$ ). Measurements will be done in controlled temperature steps varying from 25 to 70°C reflecting normal operation temperatures for solar cells. Different measurement techniques with and without the presents of series losses ( $R_s$ ) will be used to try to find how much  $R_s$  affects the different parameters.

There are very little studies to be found on the differences of  $\beta$  in the individual parameters and on what effects are contribution to which parameter. Other than one paper from 1997[11] there was not found any experimental study of the  $\beta$  for  $V_{oc}$ ,  $V_{mpp}$ ,  $I_{sc}$  and  $I_{mpp}$ . By doing these measurements and analysing the results this thesis may find trends that are different from what has previously been assumed to be true and thereby lead to more studies being done on  $\beta$ .

This investigation will be done as a step in the continued exploration of what affects the  $\beta$  of the individual parameters in a PV device. By doing real measurements of real cells experimental data can be used to further expend the knowledge in this field.

## 1.2 Research questions

- To what degree is  $\beta_{V_{oc}}$  equal to  $\beta_{V_{mpp}}$ 
  - Is this changing dependent on temperature or cell architecture
  - How much is the difference between  $\beta_{V_{oc}}$  equal to  $\beta_{V_{mpp}}$  affected by  $R_s$  in different temperatures
  - Is it the same processes affecting  $\beta_{V_{oc}}$  and  $\beta_{V_{mpp}}$
- To what degree is  $\beta_{I_{sc}}$  equal to  $\beta_{I_{mpp}}$ 
  - Is this changing dependent on temperature or cell architecture
  - How much is the difference between  $\beta_{I_{sc}}$  equal to  $\beta_{I_{mpp}}$  affected by  $R_s$  in different temperatures
  - Is it the same processes affecting  $\beta_{I_{sc}}$  and  $\beta_{I_{mpp}}$

## Chapter 2: Theory

People have always used the sun for light and heat, the sun is also responsible for the effects that produce wind and the rain on the earth. However, after humans discovered coal and oil, fossil fuels have been the easy and popular choice for energy. Later years solar energy has regained popularity much thanks higher environmental awareness, more concern for the future and a big advancement in technology[1].

### 2.1 Solar radiation

The sun is emitting vast amounts of electromagnetic radiation caused by its immense heat. Radiation emitted has different wavelengths determined by the temperature of the sun. The radiation can be seen, using Plank's radiation law, as a blackbody with a temperature of 5778K in the black line in Figure 1-1. The radiation consists mainly of short wavelength ultra violet radiation, visible light and long wavelength infrared radiation[10].

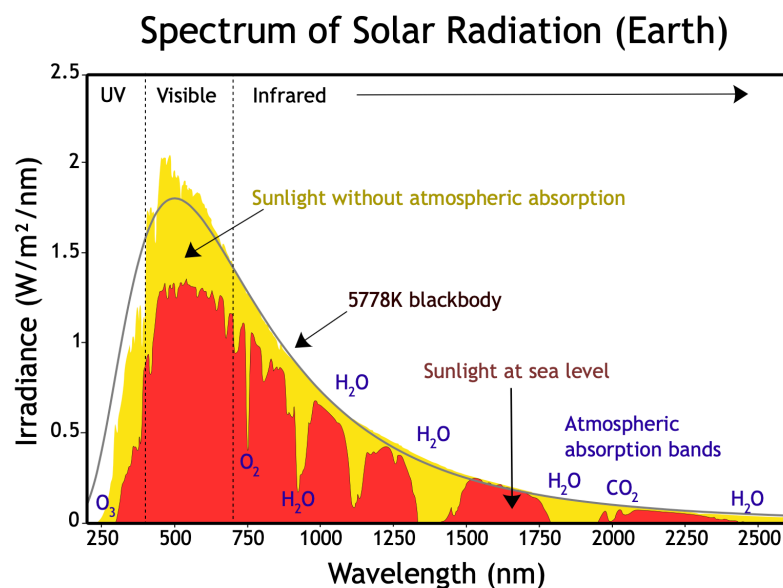


Figure 1-1 Spectrum of solar radiation [12]

The Earth's atmosphere is absorbing and scattering some of the radiation energy from the sun which means that the radiation is different at different times and locations on earth due to the relative position of the sun. Sunlight outside the earth's atmosphere has not travelled through any air and is called air mass 0 or AM0, represented by the yellow graph in Figure 1-1. Passing through the air energy from the radiation is lost. Sunlight travelling the shortest way to earth when the sun is at 90° is called air mass 1 or AM1. The standard radiation strength for PV applications is air mass 1.5, equivalent to the sun being tilted 48.2° from directly above, represented by the red field in Figure 1-1.

At AM0 the radiational energy from the sun is 1,353 kW/m<sup>2</sup>, at the standard measuring air mass AM1.5 the total power density is set to be 1,0 kW/m<sup>2</sup>. [10] The formula for approximating air mass is given as:

$$AM = \frac{1}{\cos\phi_z} \quad [2-1]$$

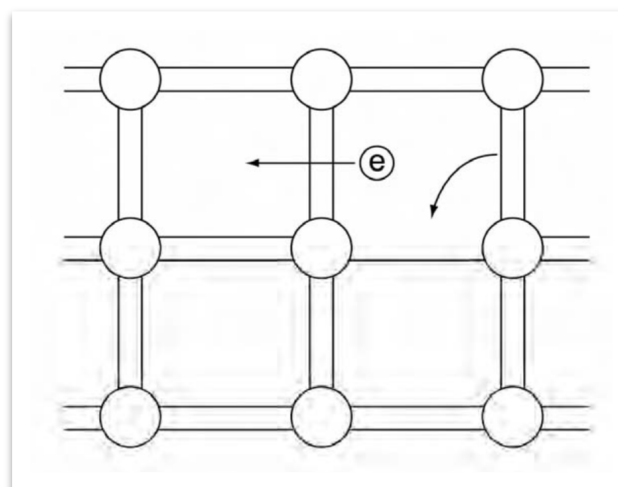
Where  $\phi_z$  is the solar zenith angle, which is the solar tilt angle from directly above.

## 2.2 Photovoltaic cells

The idea of a solar cell or a photovoltaic cell is to convert sunlight into electricity using a semiconducting material [13]. To be able to use sunlight directly for energy other than pure heat is a great advantage.

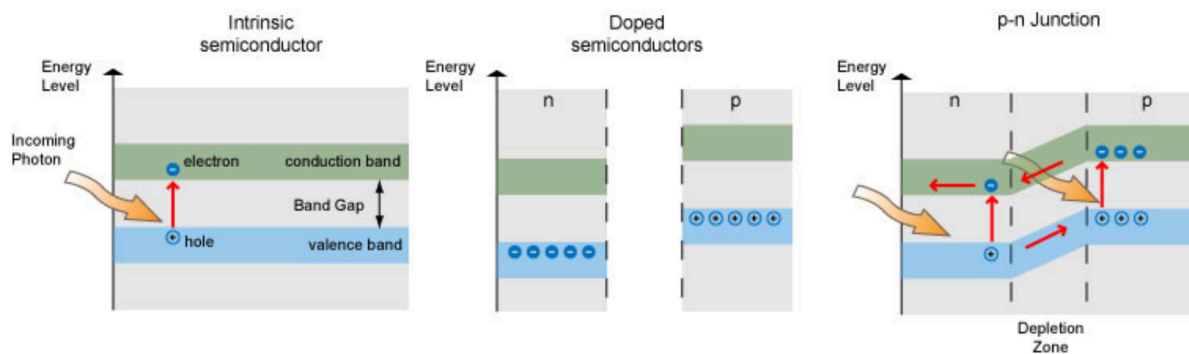
### 2.2.1 Cell material and Construction

Solar cells are made from semiconductor materials, which is materials that can act both as a conductor and an insulator dependent on the conditions. A semiconductor can change from being an insulator to a conductor when energy or heat is applied. Semiconductors have played a major role in technology and electronics since the first appearance in the invention of the AC-DC converter in 1878.[14] Semiconductor materials come from group IV or a combination of group III and V in the periodic table. The different elements have certain similarities, but also some different properties. Differences in the material properties are being exploited to make PV cells. Silicon is the most commonly used material in electronics and it is also the most used in PV technology today. [15]



Figur 2-1 Schematic representation of covalent bonds in a silicon crystal lattice. [13]

Figure 1-2 is showing a sketch of what happens when energy is applied to a silicon crystal lattice. When enough energy is applied some electron will break free from the lattice and in its place, there is now a hole. The free electron is now traveling along the lattice and the material is conducting electrons. Where the bond is broken neighbouring electrons can now break their bond and move into the hole from the free electron. This is creating what we commonly call a moving hole, moving the opposite way from the free electron. [13]

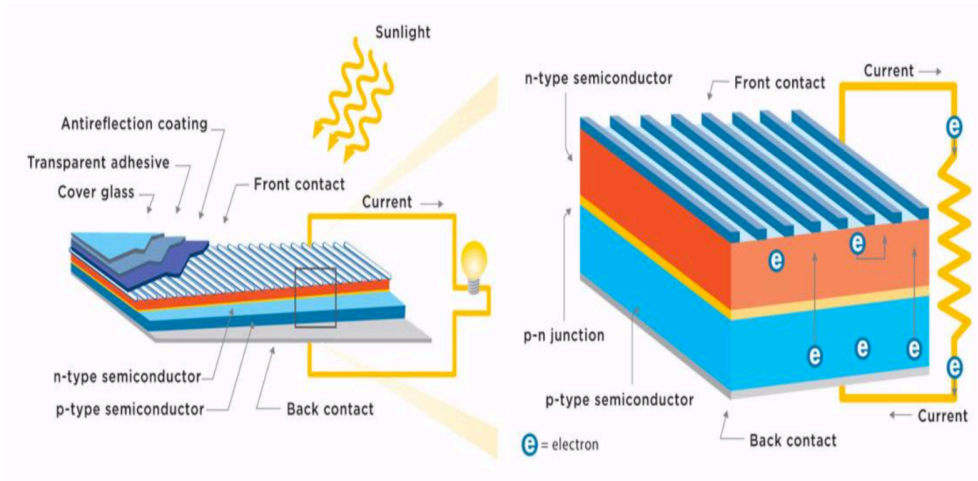


Figur 2-2 Illustration of band gap in semiconductor and a p-n junction[16, 17]

In Figure 2-2 a representation of the bandgap model of an intrinsic semiconductor and how doping affects the material to change its properties. The minimum amount of energy required for an electron to break free from its bound state is called the bandgap energy and is illustrated in the figure as a gap between the valence band and the conduction band. When an electron gets more energy than the bandgap energy the electron can be excited from the valence band to the conduction band. In the conduction band the electrons are in a free state and can move freely. The electron eventually loses the energy and drops down to the valence band, recombining with a hole. The bandgap energy varies in different materials. [10]

In the middle illustration in Figure 2-2 the effect of doping can be seen. Doping is done by adding foreign atoms in the crystal lattice with one more or one less electron than the native semiconductor atoms. When atoms with one more electron is added to the semiconductor, it is called n-type. When atoms with one less electron is introduced it is called p-type. As seen in the illustration, doping changes the energy level of the semiconductor. [10]

In the right-side illustration in Figure 2-2 the principle of a p-n junction is shown. As seen in the figure the combination of p- and n-doped semiconductor materials creates a shift in energy level between the two materials. The shift in energy between the p- and n-type materials is called the p-n junction. Electrons can when excited to the conduction band in the p-type material now have the ability to move to a lower energy level in the n-type material without dropping down to the valence band. [10]

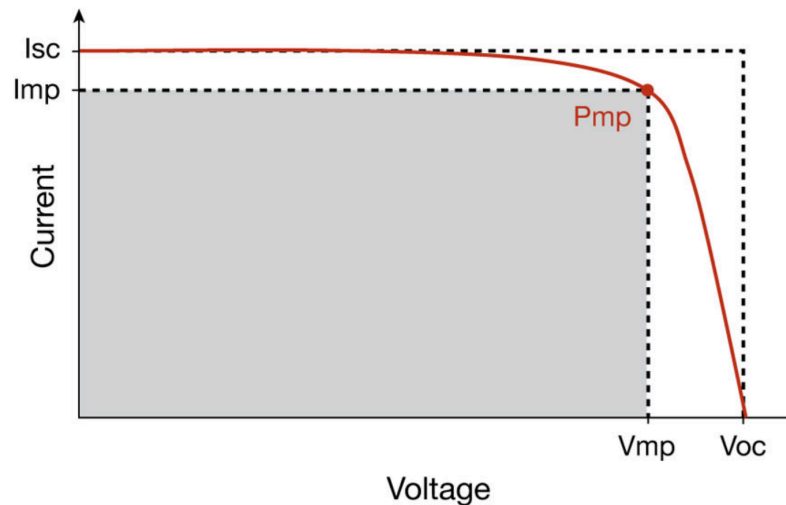


Figur 2-3 Simplified cross section view of a silicon solar cell.[18]

Figure 2-3 is an illustration of the working principles of a solar cell and its position in a solar panel. A solar panel is basically several solar cells connected together in a protective housing. In essence a PV cell is a piece of semiconducting material, normally silicon, where the bottom is doped to become a p type and the top is doped to become a n-type material. The goal is to make a large surface area to absorb more sunlight to the p-n junction to start the process seen in Figure 2-3. When sunlight hits a solar panel, the radiation penetrates the different protective layers of the solar panel and into the semiconductor materials of the cell. And as can be seen in Figure 2-2, electrons will gather on the side of the p-type and holes gather on the side of the n-type semiconductor. [10]

By connecting the n-type with the p-type semiconductor the electrons get an alternative route to recombine with the holes without going through the bandgap. As seen in figure 2-3 where the front connector and the back contact is connecting the differently doped sides of the semiconductor. The flow of electrons is creating the current and the build-up of electrons and holes on each side is what creates the voltage.[10]

## 2.3 The IV curve



Figur 2-4 Typical IV curve of a PV cell [19]

The IV curve is the most normal tool to show the characteristics of a PV cell, Figure 2-4 shows a typical IV curve for a PV cell. An IV curve is made by measuring the current (I) and the voltage (V) while adjusting the resistance from short circuit where short circuit current ( $I_{sc}$ ) is measured to open circuit, where open circuit voltage ( $V_{oc}$ ).  $I_{sc}$  and  $V_{oc}$  is the maximum I and V in a PV cell and both occurs when the other is zero. The relationship between I and V is the IV curve, the red line in the figure. Maximum power ( $P_{mp}$  or  $P_{max}$ ) is given where the product of I and V is largest, which also give the maximum power point for current and voltage ( $I_{mpp}$  and  $V_{mpp}$ ), se formula 2-2.

The maximum power produced by a PV solar cell is given as:

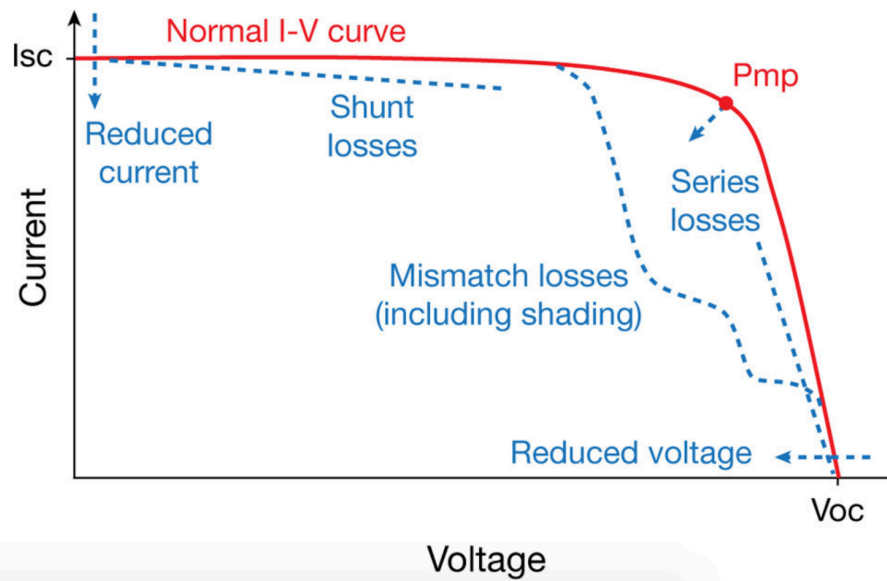
$$P_{max}(T_c) = V_{oc}(T_c) I_{sc}(T_c) FF(T_c) \quad [2-2]$$

where  $T_c$  is the cell temperature,  $V_{oc}$  is the open circuit voltage,  $I_{sc}$  is the short circuit current, FF is the fill factor. [9]

The fill factor (FF) is marked as a grey square in the figure and is given as:

$$FF = \frac{I_{mpp} V_{mpp}}{I_{sc} V_{oc}} \quad [2-3]$$

As seen in formula 2-2, all parameters for calculating the  $P_{mp}$  and therefor also  $P_{mp}$  are temperature dependent. How much each parameter varies with temperature is different and is shown in Figure 2-6.[9]



Figur 2-5 IV curve with performance impairments[19]

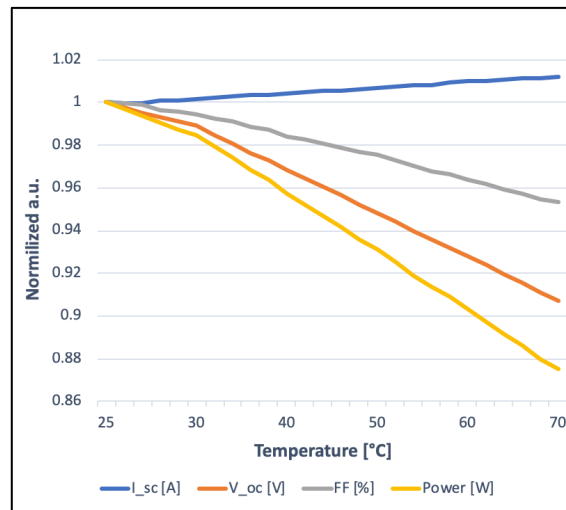
There are several losses in the PV cell, in Figure 2-5, an IV curve with five effects that reduces performance. Reduced voltage and current affect the height and width of the curve. Mismatch losses can occur scenarios like if parts or the whole panel is shaded. Shunt losses are losses from impurities in the cell material causing electrons to recombine with the holes instead of going through the circuit. Typically shunt losses are caused by a manufacturing defect.

From Figure 2-5 parameter most important to this thesis is series losses ( $R_s$ ). The  $R_s$  has three causes, movement of current through the emitter and the solar cell base, resistance in the connection between the metal contacts and the silicon and the last is resistance in the top and rear metal contacts.[20]  $R_s$  is important because it affects  $V_{mpp}$  and not  $V_{oc}$ . It is then interesting to see if it also affects the temperature dependency of  $V_{mpp}$  and nor  $V_{oc}$ .



## 2.4 Effect of temperature in silicon solar cells

Temperature has a relatively large effect on the performance of a PV cell. Higher temperatures generally yield lower performance, which is a challenge in areas with high temperatures and high solar radiation.



Figur 2-6 Correlation between cell parameters and temperature

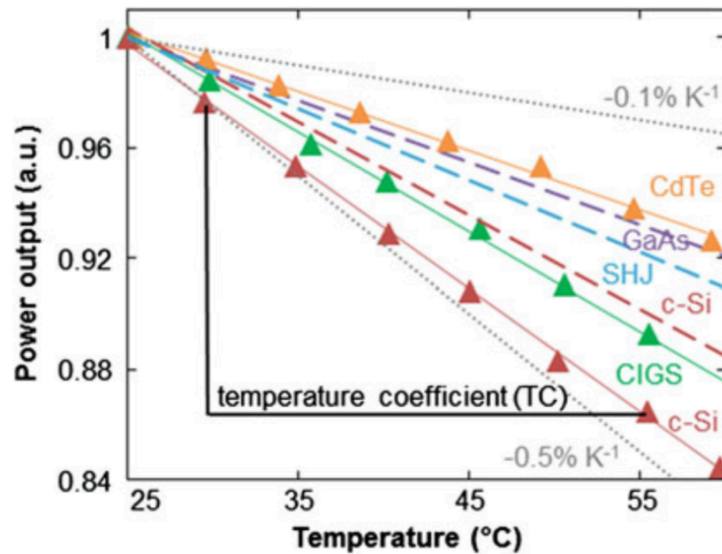
In Figure 2-6 the relationship between the parameters and temperature can be seen. From the figure it is clear that  $V_{oc}$  is the most affected by temperature change.

The linearity of the parameters makes it possible to find the temperature coefficient  $\beta$  of the maximum power by adding the  $\beta$  of the three parameters from Formula 2-2, giving following equation:

$$\beta_{P_{max}} = \beta_{V_{oc}} + \beta_{I_{sc}} + \beta_{FF} \quad [2-4]$$

where  $\beta$  is the temperature coefficient of each parameter. [9]

$\beta$  used to quantify the effect temperature has on a PV cell parameter, normally given as percentage change per degree Celsius [%/°C] or as unit part per million per Kelvin [ppm K<sup>-1</sup>] [9]. The manufacturers of PV panels usually include the  $\beta$  of the power for the panel, as a tool to contribute in the prediction of the final production of a system.  $\beta$  is an important parameter for the manufacturer to know how the PV panel will operate in different temperatures. Different types of PV cells vary differently with temperature variations which can be seen in Figure 2-7[9].



Figur 2-7 Temperature coefficients of different Photovoltaic devices[9].

## 2.5 Production of silicon solar cells

### 2.5.1 Silicon production

By far the most used material in converting solar radiation to electricity today is crystalline silicon

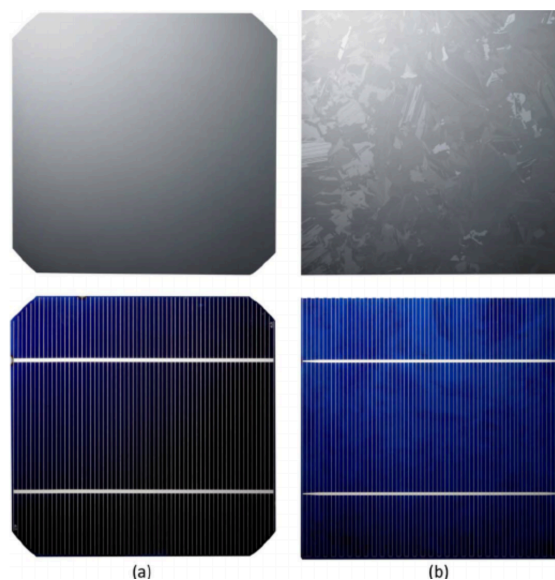
(c-Si), with 95% of the worldwide PV production[5]. The c-Si cell is a stable and well tested technology which has proven to be effective for electricity production, with record efficiencies of lab cells at 26.7% for mono-crystalline cells and 22.3 for multi-crystalline cells in 2017[6]

Silicon is luckily one of the most available elements on earth in quartz. Quartz is a combination of two chemicals, oxygen and silicon and is the most common mineral on earth. About 12 % of the land surface and 20 % of the Earth's crust is Quartz[21]. To make silicon usable for PV production it needs to be purified at least to solar-grade silicon which is 99.999% (5N) pure, typically electronic-grade silicon which is 9H pure is used in PV cells[9, 22]. The purification of silicon is done in steps, the first step is called coke reduction and is done by treating the silicon rich sand in an arc furnace which gives metallurgical grade silicon. The second step done by dissolving the silicon in Hydrogen Chloride and then a third step is either a Siemens process or a modified Siemens process to get high purity Polysilicon. The second and third step can also be done in a chemical refinement, by blowing gasses through so that the silicon melts and boron and phosphorus impurities can be removed. [23]

## 2.5.2 Cell production

The production method of the cells is influenced by several factors, such as price, time and the purity of the silicon. There are mainly two different production methods for producing crystalline silicon cells today monocrystalline (mono c-Si) and multicrystalline (mc-Si).

Mono C-Si is made by slowly pulling a rod with one silicon crystal out of a pool of melted silicon and letting the single crystal grow into a cylindrical shape. From the single crystal cylinder thin wafers are cut, the wafers are then trimmed into semi square shapes to maximize area when put in a panel. The shape is very typical for c-Si and can be seen in the (a) cell in Figure 2-8. This method creates the least amount of impurities and the final product still gives the highest efficiency in produced panels. Typically efficiency in commercial c-Si panels are in the 18-24% range, in 2012 [23].



Figur 2-8 Mono- and multi-crystalline PV cells [23]

The cells tested in this thesis are multicrystalline (mc-Si) cells made by Elkem Solar Silicon®. The process of making mc-Si wafers has undergone significant changes later years. Today ms-Si is made by casting large silicon ingots using directional solidification moulds. Ingot sizes has increased from 270kg in 2006 to ingots that are almost 2 tons in 2010. Directional solidification is achieved by controlling the temperature of the crucible as the liquid silicon is solidifying the crucible is insulated and crystals will start to form in the bottom of the mix and grow upwards. [24] This method has made it possible to cast bigger ingots yielding more wafers per ingot and thereby reducing production price. This process also contributes in purification of the silicon as impurities tend to “float” to the top of the ingot as the crystals are forming. When the ingot is hardened and cooled all sides are trimmed to remove metallic impurities that has gathered on the outside. The ingot is then cut into blocks and the blocks are cut into wafers. Mc-Si cells can be identified by the grain boundaries that forms between the different crystals in the ingot, these can be seen on cell (b) in Figure 2-8. Typically efficiency in commercial mc-Si panels are in the 14-18% range, in 2012 [23].

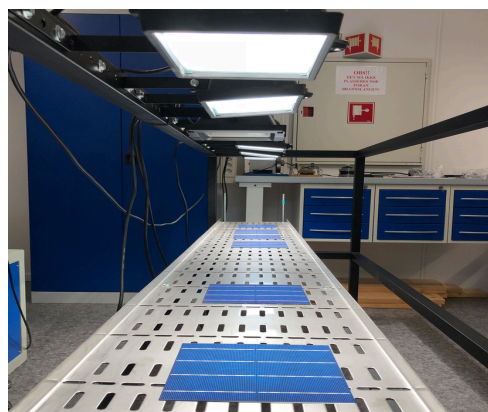
## Chapter 3: Method

In this thesis accuracy in measurements is very important to give confidence to the results. All the photovoltaic measurement data used were made in the PV Lab at University of Agder, using an IV measurement system from Neonsee. The different cells tested were examined in the same steps and with the same accuracy.

### 3.1 Light soaking

Light induced degradation (LID) is a relatively new-found phenomenon, where it is found that newly produced PV cells are changing characteristics the first few hours of being in the light. The cause of LID is not fully agreed upon yet, however there are two common theories. The first is that it is caused by metal impurities in the silicon, it is suggested that metal particles are gathering especially in the grid boundaries and then affects the parameters of the cell. The other popular theory is caused by hydrogen atoms which are introduced in the production[11]. There are already several steps in production of new cells to minimize the effect of LID. Aluminium-back surface field (Al-BSF) cells is shown to have more resistance to LID and Passivated emitter and rear cell (PERC) cells has a stronger degradation, this may be due to the passivation layers in the PERC cells prevents out diffusion.[25]

A clear truth for now is that the LID is recoverable meaning that can be stabilized by soaking the cell in light to avoid changes in performance during measurements [26]. To avoid the effect of light induced degradation all cells were light soaked in 48 hours. If it is necessary to soak the cells for 48 hours is not certain. However, 48 hours has been the norm at the PV lab for some time and then it is good to continue with the same amount of time for new cells so that they can be compared to other cells also in the local lab. There is also not found any good evidence suggesting a longer soak time for now. The light soaking rig, see Figure 3-1, consists of six lamps which are spreading an even light to a shelf where the PV cells are placed. Each lamp is installed with a 400W light bulb that provides plenty of light and heat for the cells. Cells are spread evenly so that one cell have one lamp right above.



Figur 3-1 Light soaking rig at the UiA PV lab

## 3.2 Measurements

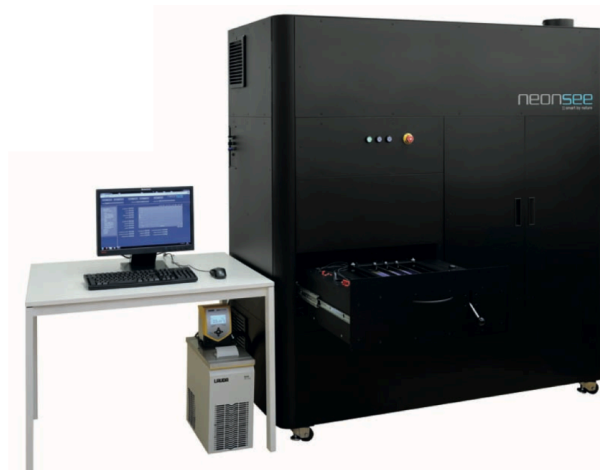
### NeonSee BIV-HCSS-21

The sun simulator used for all measurements was a NeonSee AAA sun simulator see Figure 3-2. The NeonSee device uses a testing tray with capacity of one cell at a time, the cell is secured using vacuum pressure creating a near perfect connection between the copper connector and the back of the cell. Probes are connected to the busbars on top of the cell. The two different types of cells tested in this thesis is Al-BSF and PERC cells. The Al-BSF cell have three busbars in the front and the machine is then set up with three rows of 15 probes connecting the front of the cell, while the PERC cell has four rows of busbars and is thus set up with four rows of probes. The temperature of the cell is measured by a PT100 thermometer which has the probe located in the middle of the brass plate. The machine uses a heat pump to control temperature by pumping hot or cold water through the copper plate. Practical operating temperatures is between 19°C and 70°C.

### 3.2.1 Calibration

The sun simulator is calibrated with a calibration cell every time it is started to insure consistent measurements. Both calibration routines are done in Standard Test Conditions (STC) IEC 60891, listed below. The calibration process is first to calibrate the irradiance twice with a minimum of 15min in between to ensure that the lamp is stable and to ensure that the system is fully warmed up. When the calibration is run the operator tries to keep the desired temperature is within a  $\pm 0.2^\circ\text{C}$  of the STC. The second calibration is the Irradiance vs Attenuator is calibrated with the same temperature accuracy. The attenuator is a mechanical pumper which can adjust the irradiance from the lamp and the tested cell. The attenuator operates between full opening where the cell is hit with the full  $1000\text{W}/\text{m}^2$  to minimum which is practically  $0\text{W}/\text{m}^2$ .

Standard test conditions	STC
Cell temperature	25°C
Irradiance	1000 W/m <sup>2</sup>
Air mass	1.5
Wind Speed	0m/s



Figur 3-2

Sun simulator : NeonSee BIV-HCSS-21 [27]

### 3.2.2 Accuracy

To create accurate and consistent data the selected cells are measured using three different methods which measures the cells slightly differently. Measuring with different methods makes it possible to look at the consistency of the results and can also give an indication of the validity of the results. The difference in measuring methods is both in software differences and in measuring hardware. Software controlled differences is things like temperature triggers and temperature control for the different methods. Hardware differences is that in some of the measuring techniques some of the parameters can be calculated or they can be measured directly in the sun simulator. There are advantages to the different methods and since different methods can be used to find the same parameters this can be a good indication to whether the results of one technique is valid or not.

### 3.2.3 Temperature scan

For every PV cell measured a temperature scan (Tscan) is done to make IV measurements for temperatures from 25°C to 70°C with a high temperature accuracy. The Tscan measurement technique is for this thesis set to take an IV measurement automatically for every one or two degree increase in temperature from 25°C to 70°C. A total of 30 IV curves are taken every Tscan. In addition, backup measurements are also taken when the cell is cooled, this way there is a total of 60 IV measurements taken every Tscan. The Tscan data is important in this thesis because it gives I and V data with  $R_s$ , which will be compared to Suns-Voc and Isc-Voc data without  $R_s$ .

### 3.2.4 Suns -Voc and Isc – Voc

The reason for using Suns – Voc and Isc – Voc measurements are to get IV curves without  $R_s$ . This is done by varying the illumination of the tested cell and measuring Isc and Voc at every illumination level. The difference between Suns-Voc and Isc-Voc is that Suns-Voc uses a light sensor to calculate current by measuring the changing illumination, while Isc-Voc directly measures current from the cell. The Suns-Voc is not affected by  $R_s$  since no current is pulled from the cell. For Isc-Voc measurements Isc is not affected by  $R_s$  so long as the it is not bigger than  $10\Omega\text{cm}^2$ .

Suns – Voc and Isc – Voc measurements are taken from every cell at temperatures 25°C, 35°C, 45°C, 55°C and 65°C. A combined measurement of Suns-Voc and Isc-Voc took on average seven minutes per temperature step, while the lamp starts at 1000 W/m<sup>2</sup> and ends with 0 W/m<sup>2</sup>. This time per measurement and the changing heat from the lamp makes it difficult to maintain a desired temperature. Temperature stability is especially difficult at the higher temperatures where the ambient air is contributing in cooling the machine whole the lamp is on low illumination. To have reliable results for measurements there was taken three measurements for each temperature step for every cell. For the three measurements small changes were done to get the temperature as close to target temperature as possible.

### 3.2.5 Lab time and routines

For a good investigative analysis, which was the aim for this thesis, it is important to make a good lab routine and make the measuring repeatable so that they can be reproduced by others. A lot of time was spent in the beginning to find a repeatable routine for measuring many cells. Investigation in which measuring techniques to be used had to be done and it was important to find the right set of cells to get a good spread of results.

Calibration of the sun simulator was done repeatedly until desired accuracy was achieved for every cell. All the cells were measured the same way with the same treatment before. This meant that it was not possible to measure more than one cell in one work day. Some cells also had to be measured more than once due to insufficient accuracy found in the results or because of errors in the sun simulator software.

The NeonSee although a class AAA sun simulator is from a relatively small company who have their main focus set for industry. This means that guidance to the simulator is hard to get and trial and error mixed with accumulated experience has been the way to figure out the right procedure. There is also little information about the inside of the machine and software which makes it hard to know exactly what is happening in each measurement.

### 3.2.6 Cells tested

All three sets of tested cells are produced from high grade mc-Si by Elkem Solar. To get some spread of results for comparing while still focusing more on quality in the results than quantity three different sets of cells were chosen with two slightly different technology. Two of the sets of cells are PERC cells, the difference is that they were made from two different ingots. One ingot was made a target resistivity of  $0.5 \Omega$ , cells from this ingot is later called PERC 0.5 cells, the other ingot was made with a target resistivity of  $1.3 \Omega$ , these cells are later called PERC 1.3 cells. The last set of cells is of a slightly different kind of mc-Si cells, Al-BSF cells.

For all three sets of cells the cell number was chosen with as close of a spread to each other as possible. The cell number represents its placement in the ingot it was cut from. The numbers for both the Al-BSF and the PERC cells are written on the following form: XXXX – XX – XXX. The first four numbers correspond to the id of the ingot which is the uncut slab of silicon from the crucible, the second two numbers correspond to the block which is cut from the ingot, these are cut to the right length and width for a cell, the last number corresponds to the position in the cell had in the block when it was cut into thin wafers. The most interesting for this thesis is the last number, where low numbers indicate a low placement in the block. The position is interesting due to the difference in cell architecture through the ingot. A table of the cells tested can be seen on the next page.

AI-BSF	PERC 0.5	PERC 1.3
2099-07-005	3645-22-003	3643-22-003
2099-07-009	3645-22-012	3643-22-008
2099-07-012	3645-22-022	3643-22-013
2099-07-022	3645-22-031	3643-22-022
2099-07-027	3645-22-041	3643-22-041
2099-07-034	3645-22-052	3643-22-052

Tabell 3-1 All the tested cells

The number of times each cell was tested has some variation due to priority of importance and time. The Tscan was performed once for each cell, Suns-Voc and Isc-Voc was performed once per AI-BSF cell and three times per PERC 0.5 and PERC 1.3 cell. This is what is used for the further calculation and analysis. Some cells had to be measured more times because of error or inaccuracy in the measurements, however the number of tests used is the one stated before.

The reason for doing three measurements per temperature per cell for Suns-Voc and Isc-Voc was to get better data for error analysis and to get some indication of the accuracy of the sun simulator measurements and the calibration process. For the AI-BSF cells the temperatures were more stable than for the PERC cells and the results showed good linearity and low errors therefore one measurement per temperature per cell were considered sufficient. The Tscan measuring technique takes 30 measurements per tested cell from 25 to 70°C. With this volume of data, one test using Tscan per cell were considered sufficient.

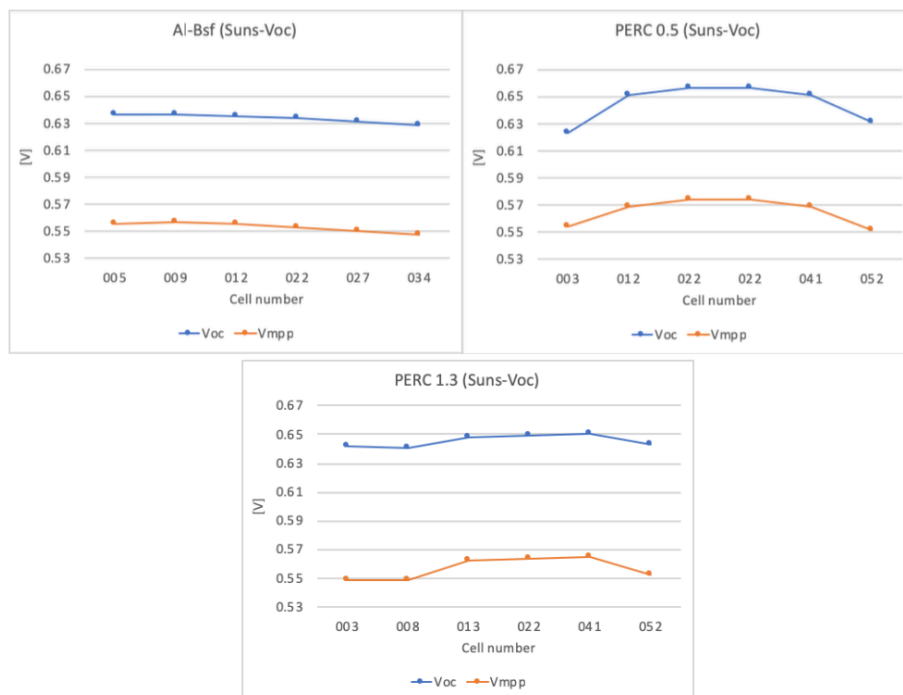


Figure 3-3 Voc and Vmpp in STC for each cell for A-BSF, PERC 0.5 and PERC 1.3

To see the effect of the ingot position Figure 3-3 show comparison between Voc and Vmpp done in STC. The data used are measured with Suns-Voc, however Tscan and Isc-Voc gave identical results. As can be seen from the figure, the variation is different both from the different stack of cells and for the individual cells in each selection.

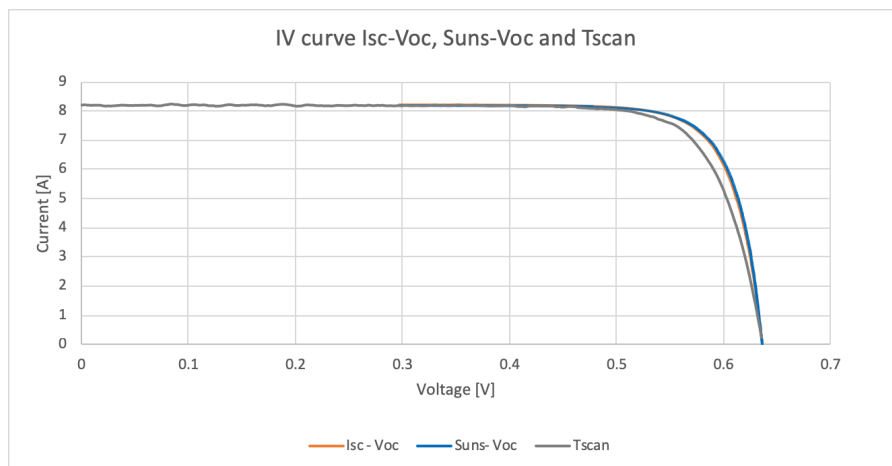


### 3.3 Data analysis

Measurement data from the sun simulator comes as txt files which is treated in excel to calculate the parameters necessary. In the analysis the differences of the three measuring techniques, Suns-Voc, Isc-Voc and Tscan, described previously is taken advantage of. One of the main goals in this thesis is to see how much of an effect  $R_s$  has on the PV cell. This may be possible to observe by comparing results from Suns-Voc and Isc-Voc with Tscan. Since all the tests were done in the same environment, it can be assumed that any major differences may be from the  $R_s$ .

#### 3.3.1 Comparison between IV curve measurements

In the analysis the first step taken was to test the accuracy of measurements. The three different measurement techniques have different technical methods to gather much the same data. To be sure that the final results are correct the early data should be controlled against the different measurements.

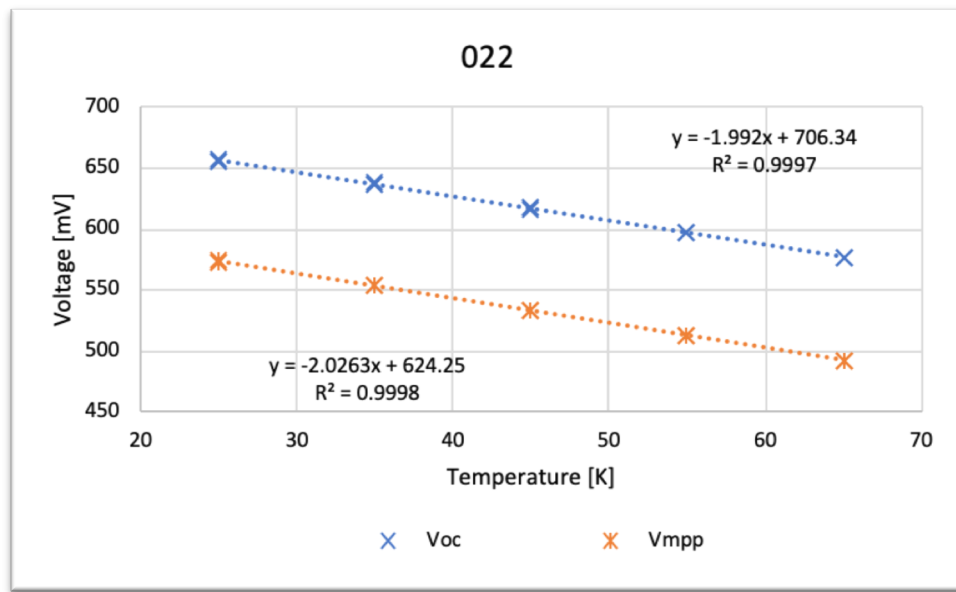


Figur 3-4 Isc-Voc, Suns-Voc and Tscan, IV comparison for 2099-07-005

As seen in Figure 3-4 the IV curves generated from data by Suns-Voc and Isc-Voc, displayed in orange and blue, is virtually identical, while the Tscan curve in grey is slightly lower. The results are satisfying in ensuring that measurements for Suns-Voc and Isc-Voc is more or less identical while Tscan data is slightly lower due to the series resistance  $R_s$ . Figure 3-4 is from cell 2099-07-005 which is one of the Al-BSF cells.

### 3.3.2 Temperature coefficients

The main goal of the thesis is to compare temperature coefficients from some chosen parameters. Namely testing the if there was a difference in  $\beta$  and if there is when it occurs between  $V_{oc}$  and  $V_{mpp}$  and  $I_{sc}$  and  $I_{mpp}$ . Temperature coefficient, as explained in Chapter 2, is a way to quantify how much temperature is affecting the parameter looked at. This is why several temperatures had to be measured for each cell.



Figur 3-5 Suns-Voc measured Voltage per temperature for cell 3645-22-022

The example in Figure 3-5 shows the voltage data in mV with temperature ranging from 25°C to 65°C, from cell 3645-22-022, taken using Suns-Voc measurement technique. The points on the curves each represents three measurements taken for  $V_{oc}$  and  $V_{mpp}$ . From the figure it can be seen the three measurements are very close, this gives a good indication of accuracy of the machine and of the measurements.

The coefficient of determination ( $R^2$ ) quantifies the linearity of the trendline. If  $R^2$  is 1 the line is perfectly linear. In Figure 3-5 the dotted line is the trendline for all data points, which here is a linear regression of the data points with  $R^2=0.9997$  and  $0.9998$ , which suggest that the results are accurate data is reliable.[28] Accuracy in the measurements also indicates that the calibration process is reliable.

Effectively the  $\beta$  is the slope of a curve when the curve is for a parameter over several temperatures. In Figure 3-5 the equation for each curve is given as:

$$y = mx + b \quad [3-1]$$

where  $m$  is the slope of the curve and  $b$  is the value of  $y$  when  $x=0$ . In this example the  $\beta$  is  $-0.992$  mV/K for  $V_{oc}$  and  $-2.0263$  mV/K for  $V_{mpp}$ . Since these numbers are in millivolts and the results are so close further and more accurate treatment of the data was needed.

### 3.3.3 Plotting temperature coefficients using LINEST

To get accurate results for  $\beta$  it is directly calculated using the LINEST function in excel following Professor Faith A. Morrison's paper on "*Obtaining Uncertainty Measures on Slope and Intercept of a Least Squares Fit with Excel's LINEST*" [29]. The LINEST function returns an array of ten statistics about the selected set of paired  $(x_i, y_i)$  data. The slope in the LINSET array is made using this equation for the least squares estimator of the slope:

$$\hat{m} = \frac{n \sum_{i=1}^n x_i y_i - (\sum_{i=1}^n x_i)(\sum_{i=1}^n y_i)}{n \sum_{i=1}^n x_i^2 - (\sum_{i=1}^n x_i)^2} = \frac{SS_{yx}}{SS_{xx}} \quad [3-2]$$

where  $\hat{m}$  is the slope of gradient,  $x$  is the temperature data,  $y$  is the voltage data,  $S_{y,x}^2$  is the standard deviation of  $y(x)$  and  $SS_{yx}$  is the sum of squared error between the data and the mean of the data.

The error is also found by the standard deviation of slope in the LINSET by using following equation:

$$S_m^2 = \frac{S_{y,x}^2}{SS_{xx}} \quad [3-3]$$

where  $S_m$  is the standard deviation of slope  $\hat{m}$ . The rest of the functions in the LINSET array is not used in this thesis.

The results for standard deviation of slope are important when comparing the  $\beta$  with each other, because when comparing two parameters it is important to know the error of the measurements. The standard slope of deviation will be presented as error bars for all  $\beta$  data in the next chapter.

## Chapter 4: Results and discussion

In this chapter the main focus is comparing temperature coefficients ( $\beta$ ) of different parameters, first between  $V_{oc}$  and  $V_{mpp}$  in Chapter 4.1 and then between  $I_{sc}$  and  $I_{mpp}$  in Chapter 4.3. The error bars are made from calculating the standard deviation of the slope of each parameter, explained in Chapter 3.

### 4.1 $V_{oc}$ and $V_{mpp}$ temperature coefficient

Results in the following chapter displayed as absolute values for  $\beta$  in [mV/K]. The Y-axis limits are set to be the same for each set of results to make comparison easier between the different measurement techniques.

In all the figures in this chapter the different  $\beta$  parameters are displayed as following,  $\beta_{V_{oc}}$  is shown as green triangles with green error bars,  $\beta_{V_{mpp}}$  is shown with a red X and red error bars. Tscan results are shown in blue squares for  $\beta_{V_{oc}}$  and as blue triangles for  $\beta_{V_{mpp}}$ . For each set of different type cells tested Suns- $V_{oc}$  and  $I_{sc}$ - $V_{oc}$  measurement methods have their own Figure: (a) and (b). In both Suns- $V_{oc}$  (a) and  $I_{sc}$ - $V_{oc}$  (b) figures Tscan data is displayed to be analysed and as a comparison for  $\beta$  with and without  $R_s$ . This way it is possible to analyse results from Suns- $V_{oc}$  and  $I_{sc}$ - $V_{oc}$  separately and in comparison, to each other and to Tscan results.

#### 4.1.1 AI-BSF cells

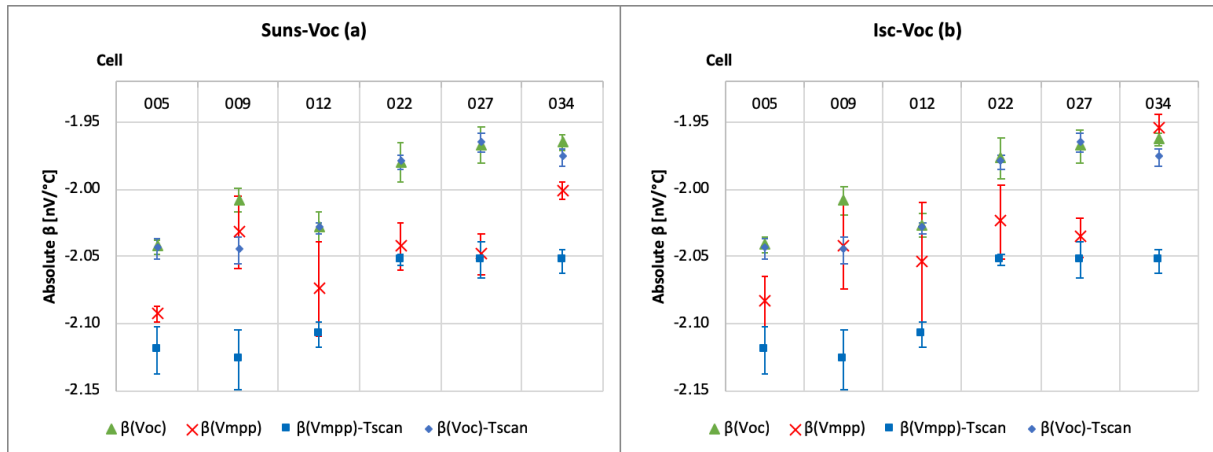


Figure 4-1 (a) and (b) AI-BSF  $\beta$  for Voc and Vmpp

Figure 4-1 is presenting  $\beta_{V_{oc}}$  and  $\beta_{V_{mpp}}$  from six AI-BSF cells measured using Suns-Voc and Tscan in Figure 4-1(a) and using Isc-Voc and Tscan in Figure 4-1(b).

For the Tscan results displayed in both Figure 4-1 (a) and (b),  $\beta_{V_{oc}}$  and  $\beta_{V_{mpp}}$  are statistically different. Which here means that all the tested cells show higher values for  $\beta_{V_{oc}}$  than for  $\beta_{V_{mpp}}$ , and there is no overlap in the standard deviation. For the Tscan results the difference between  $\beta_{V_{oc}}$  and  $\beta_{V_{mpp}}$  is similar for all the cells, ranging between 0.073mV/K for cell 022 and 0.087mV/K in cell 027. There is also a rise in value for both  $\beta_{V_{oc}}$  and  $\beta_{V_{mpp}}$  in the three higher numbered cells, with a small ramp up in cell 012. Cell 005 and 009 have slightly higher standard deviation in  $\beta_{V_{mpp}}$  than the rest of the Tscan results.

For the Suns-Voc results displayed in Figure 4-1 (a), the trend is that  $\beta_{V_{oc}}$  and  $\beta_{V_{mpp}}$  are statistically different, where all tested cells show higher values for  $\beta_{V_{oc}}$  than for  $\beta_{V_{mpp}}$ . Most of the cells also have no overlapping of the standard deviation the exceptions are cell 009 and 012.  $\beta_{V_{oc}}$  results from Suns-Voc is virtually identical to  $\beta_{V_{oc}}$  results from Isc-Voc shown in Figure 4-1(b). The  $\beta_{V_{oc}}$  is also the same value within standard deviation for both Tscan and Suns-Voc results, except for cell 009, where  $\beta_{V_{oc}}$  is slightly higher for the Suns-Voc result. Some noticeable differences in the Suns-Voc results, cell 009 and 034 have smaller difference between  $\beta_{V_{oc}}$  and  $\beta_{V_{mpp}}$ , also cell 012 have a significantly larger standard deviation for  $\beta_{V_{mpp}}$  compared to the rest of the cells.

For the Isc-Voc results displayed in Figure 4-1 (b), the trend is that  $\beta_{V_{oc}}$  and  $\beta_{V_{mpp}}$  are different, where all tested cells show higher values for  $\beta_{V_{oc}}$  than for  $\beta_{V_{mpp}}$  except of cell 034, where the opposite is true. Since  $\beta_{V_{oc}}$  from Suns-Voc are almost identical to  $\beta_{V_{oc}}$  from Isc-Voc, the connection is also the same between  $\beta_{V_{oc}}$  results from Tscan and Isc-Voc. Compared to the Suns-Voc data,  $\beta_{V_{mpp}}$  is slightly larger and the standard deviations are larger, making the distinction between  $\beta_{V_{oc}}$  and  $\beta_{V_{mpp}}$  less clear for the Isc-Voc results. Some noticeable differences in the Isc-Voc results, cell 034 shows a  $\beta_{V_{mpp}}$  slightly larger than  $\beta_{V_{oc}}$ , also cell 012 have a significantly larger standard deviation for  $\beta_{V_{mpp}}$  compared to the rest of the cells.

### 4.1.2 PERC 0.5 cells

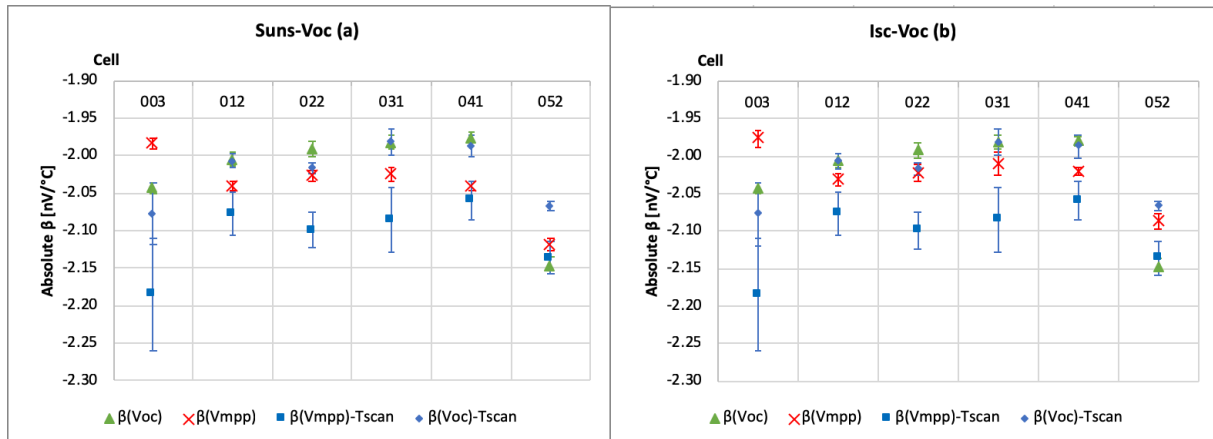


Figure 4-2 (a) and (b) PERC 0.5  $\beta$  for  $V_{oc}$  and  $V_{mpp}$

Figure 4-2 is presenting  $\beta_{V_{oc}}$  and  $\beta_{V_{mpp}}$  from six Al-BSF cells measured using Suns-Voc and Tscan in Figure 4-2(a) and using Isc-Voc and Tscan in Figure 4-2(b).

For the Tscan results displayed in both Figure 4-2 (a) and (b), the trend is that  $\beta_{V_{oc}}$  and  $\beta_{V_{mpp}}$  are statistically different. Which here means that all the tested cells show higher values for  $\beta_{V_{oc}}$  than for  $\beta_{V_{mpp}}$ , and except of cell 003 there is no overlap in the standard deviation. A rise in  $\beta_{V_{oc}}$  value can be seen in the higher numbered cells except for cell 052. Cell 003 has significantly higher standard deviation in  $\beta_{V_{mpp}}$  than the rest of the Tscan results, 003 is also the only cell where the standard deviation is overlapping between  $\beta_{V_{oc}}$  and  $\beta_{V_{mpp}}$ .

The Suns-Voc results displayed in Figure 4-2 (a) are practically identical to the results from Isc-Voc displayed in Figure 4-2 (b), the only noticeable difference is that  $\beta_{V_{mpp}}$  from Isc-Voc is slightly larger than  $\beta_{V_{mpp}}$  from Suns-Voc. The following comments will therefore be for both Suns-Voc and Isc-Voc. The results display a statistical difference between  $\beta_{V_{oc}}$  and  $\beta_{V_{mpp}}$ , in that there is no overlapping between the two for any of the cells. For the four cells in the middle  $\beta_{V_{oc}}$  and  $\beta_{V_{mpp}}$  are very close in value with  $\beta_{V_{oc}}$  slightly larger. Both cell 003 and 052 is different than the rest since  $\beta_{V_{mpp}}$  is larger than  $\beta_{V_{oc}}$ . In cell 003  $\beta_{V_{mpp}}$  is noticeably large and in cell 51 both  $\beta_{V_{oc}}$  and  $\beta_{V_{mpp}}$  are noticeably small compared to the other cells.

### 4.1.3 PERC 1.3 cells

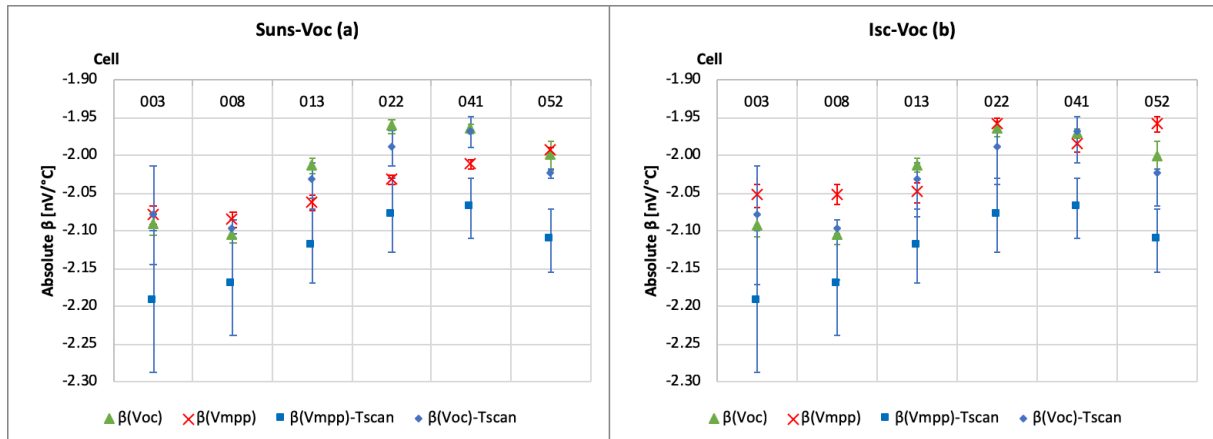


Figure 4-3 (a) and (b) PERC 1.3  $\beta$  for Voc and Vmpp

Figure 4-3 is presenting  $\beta_{Voc}$  and  $\beta_{Vmpp}$  from six PERC 1.3 cells measured using Suns-Voc and Tscan in Figure 4-3(a) and using Isc-Voc and Tscan in Figure 4-3(b).

For the Tscan results displayed in both Figure 4-3 (a) and (b),  $\beta_{Voc}$  and  $\beta_{Vmpp}$  all the tested cells show higher values for  $\beta_{Voc}$  than for  $\beta_{Vmpp}$ , however in four of the six cells the standard deviation is overlapping. For the Tscan results the difference between  $\beta_{Voc}$  and  $\beta_{Vmpp}$  is similar for all the cells, but the standard deviation is varying for the different cells and is largest for cell 003.

For the Suns-Voc results displayed in Figure 4-3 (a), there are two trends, in cells 013, 022 and 041,  $\beta_{Voc}$  and  $\beta_{Vmpp}$  are statistically different, which here means that all the tested cells show higher values for  $\beta_{Voc}$  than for  $\beta_{Vmpp}$  and there is no overlapping in standard deviation. The other trend in the Suns-Voc results is for cell 003, 008 and 052, where  $\beta_{Vmpp}$  is slightly larger than  $\beta_{Voc}$  and the standard deviations of the two is overlapping making them practically the same values.

For the Isc-Voc results displayed in Figure 4-3 (b), the results differ from cell to cell. For cell 003, 008, 013 and 052,  $\beta_{Voc}$  and  $\beta_{Vmpp}$  can be seen as statistically different, since there is no overlap between the standard deviation for any of the cells. For cell 003, 008 and 052,  $\beta_{Vmpp}$  is larger than  $\beta_{Voc}$ , while the opposite is true for cell 013. The remaining two cells, 022 and 041, the values are practically the same for  $\beta_{Voc}$  and  $\beta_{Vmpp}$ .

A general trend for all three measuring techniques in Figure 4-3 (a) and (b) is that all values for  $\beta_{Voc}$  and  $\beta_{Vmpp}$  is rising with the cell numbers from 003 to 041 and falls slightly at cell 052.

## 4.2 Discussion for Voc and Vmpp measurements

The reason for measuring Voc and Vmpp and calculating  $\beta_{Voc}$  and  $\beta_{Vmpp}$  was to investigate the main question in this thesis, “is  $\beta_{Voc}$  equal to  $\beta_{Vmpp}$ ”. While reason for having  $\beta$ -data from Suns-Voc and Isc-Voc in the same figures as  $\beta$ -data from Tscan is to investigate the other part of the question, “How much is Rs affecting the difference between  $\beta_{Voc}$  and  $\beta_{Vmpp}$ ”.

Results from the Tscan measuring  $\beta$  with Rs is perhaps the most relevant results since Rs already is a part of the PV cell and results with Rs can be more relatable to PV cells in industry. The results from Suns-Voc and Isc-Voc measuring  $\beta$  without Rs is made more to compare with the Tscan results to possibly be able to say something about the effect of Rs to the different  $\beta$  parameters.

For the majority of the  $\beta_{Voc}$  and  $\beta_{Vmpp}$  results for all the cells, Suns-Voc and Isc-Voc methods produce similar results. This is closest in the results for  $\beta_{Voc}$  where most cells show a virtually identical value for the two methods. There are small variations in  $\beta_{Vmpp}$  for most cells, which probably is caused by the different techniques being used to measure current. I consider the Isc-Voc results as the most accurate and realistic for the tested cell, because Isc-Voc is measuring the current directly from the tested cell, whereas the Suns-Voc uses a separate sensor to calculate the current mentioned in chapter 2.7.

The results from the Tscan measuring shows a trend that there is a statistically significant difference between  $\beta_{Voc}$  and  $\beta_{Vmpp}$ . In all the tested Al-BSF cells,  $\beta_{Voc}$  was higher  $\beta_{Vmpp}$  with no overlapping in the standard deviation. The same result was observed for the two other types of cells, except of PERC 0.5 cell number 003 and PERC 1.3 cells 003 and 013, where the standard deviation of the slopes overlapped, and the parameters cannot be described as statistically different. There is still a clear indication that there may be a difference in  $\beta_{Voc}$  and  $\beta_{Vmpp}$  from the Tscan results, however with the small sample sizes and low number of measurements the standard deviation may change.

For  $\beta_{Voc}$  and  $\beta_{Vmpp}$  measured using Suns-Voc and Isc-Voc methods the trends are less clear than for Tscan. One of the observations that can be seen is that for the Tscan results of each set of cells the difference between  $\beta_{Voc}$  and  $\beta_{Vmpp}$  is relatively similar from cell to cell, however this is not the case for Suns-Voc or Isc-Voc. For both methods most of the cells shows that  $\beta_{Voc}$  is larger than  $\beta_{Vmpp}$ , however this is not consistent, and the standard deviation of each cell is also varying relatively much.

One assumption was that  $\beta_{Vmpp}$  is affected by Rs, logically if this was the only parameter affecting, then  $\beta_{Vmpp}$  would be equal to  $\beta_{Vmpp}$  for the Suns-Voc and Isc-Voc measurements which are not affected by Rs. This is however typically not the trend in the results, indicating that Rs is not the only parameter affecting  $\beta$ . By there being a majority of cells showing a trend where  $\beta_{Voc}$  is similar and  $\beta_{Vmpp}$  is different between the measuring techniques with and without the Rs, there is an indication that Rs is affecting  $\beta_{Vmpp}$ . The extent of the effect from Rs is uncertain due to the lack of consistency for the  $\beta_{Vmpp}$  results between the different measurement techniques, other than  $\beta_{Vmpp}$  generally having lower values in the Tscan results.



For the three different measurement techniques there is a trend showing higher values for both  $\beta_{Voc}$  and  $\beta_{Vmpp}$  in the higher numbered cells. This trend is seen strongest in the Al-BSF and the PERC 1.3 cells, for the PERC 0.5 cells this effect is a bit less prominent. For both set of PERC cells the highest numbered cell has lower value for  $\beta_{Voc}$  and  $\beta_{Vmpp}$  than the second highest. This trend was expected and is showing some of the effect different positions in the silicon block have on the wafers. As mentioned earlier each cells number is correlating with the position it had in the silicon block, lower numbers indicate a lower position in the block. The position in the block gives slightly different cell architecture which is as seen here affecting performance of the cell.

The  $\beta$  results for Voc and Vmpp are displayed in mV/K which is a very small unity, however it is important to remember that this is measurements for single PV cells. If the STC Voc=650mV for one cell and there are generally around 60 cells per panel then 2mV/K can mean a lot for a system. As a scale the difference between  $\beta$  from Voc and Vmpp is in most of the cells making less of an impact to the potential of the cell than the position of the wafer in the silicon block. The maximum spread in  $\beta$  between  $\beta_{Voc}$  and  $\beta_{Vmpp}$  for all six cells and all three measuring techniques with standard deviation added is 0.18mV/K for Al-BSF, 0.29mV/K for PERC 0.5 and 0.34mV/K for PERC 1.3. Meaning that practically the difference in between  $\beta_{Voc}$  and  $\beta_{Vmpp}$  is perhaps leading to little change in the produced cells today. However, the goal of the thesis is more to do an experimental investigation to contribute to the research of the effect of temperature on silicon solar cells.

A lot of the result analysis and assumptions of the different trends given for the tested parameters are affected by the standard deviation of the slope of each tested parameter. The method used to calculate the standard deviation of slope is explained in Chapter 3.3.3. This standard deviation is basically stating how much the data varying from each other and how much they vary from a straight line, which tells something about the spread in the data and the certainty of the measurements. For all results standard deviation is projected by error bars in the parameters colour. From cell to cell the error bars are varying in size for all measurement techniques. The number of measurements per temperature per cell and the temperature interval of measurements affect how reliable the results are, the amount of measuring for this thesis is explained in Chapter 3.2.5. Realistically the assumptions made here is based on the certainty of the measurements done which may give some variations in the results with more work in the lab.

The fact that the standard deviation for both sets of PERC is noticeably smaller than for the Al-BSF cells in the Suns-Voc and the Isc-Voc results is very positive for the confidence in the measured data. This is because the cells that are tested three times per temperature step is showing lower standard deviation than the cells tested once per temperature step.

### 4.3 Isc and Imppp temperature coefficient

Results in the following chapter displayed as Absolute values for  $\beta_{Isc}$  and  $\beta_{Imppp}$  in [mA/°C]. The Y-axis limits are also set to be the same for all figures to make the comparison easier. The values for current from the sun simulator are presented as negative values, therefore all of the results for current has been corrected by multiplying with -1. As explained in Chapter 2,  $\beta$  for current is positive.

In all the figures in this chapter the different  $\beta$  parameters are displayed as following,  $\beta_{Isc}$  is shown as green triangles with green error bars,  $\beta_{Imppp}$  is shown with a red X and red error bars. Tscan results are shown in blue squares for  $\beta_{Isc}$  and as blue triangles for  $\beta_{Imppp}$ . For each set of different type cells tested Suns-Voc and Isc-Voc measurement methods have their own Figure: (a) and (b). In both Suns-Voc (a) and Isc-Voc (b) figures Tscan data is displayed to be analysed and as a comparison for  $\beta$  with and without  $R_s$ . This way it is possible to analyse results from Suns-Voc and Isc-Voc separately and in comparison, to each other and to Tscan results.

#### 4.3.1 Al-BFS cells

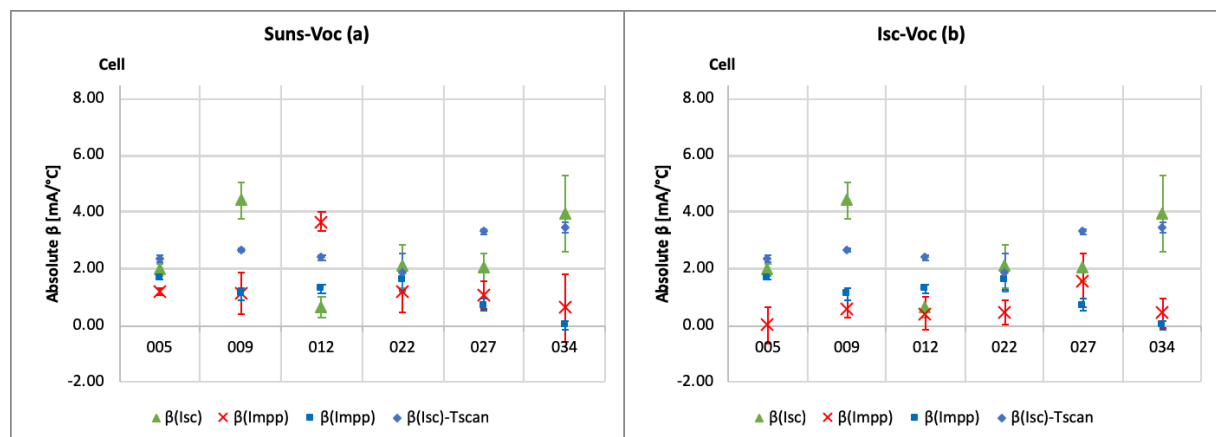


Figure 4-4 (a) and (b) Al-BSF  $\beta$  for Isc and Imppp

Figure 4-4 is presenting  $\beta_{Isc}$  and  $\beta_{Imppp}$  from six Al-BSF cells measured using Suns-Voc and Tscan in Figure 4-4(a) and using Isc-Voc and Tscan in Figure 4-4(b).

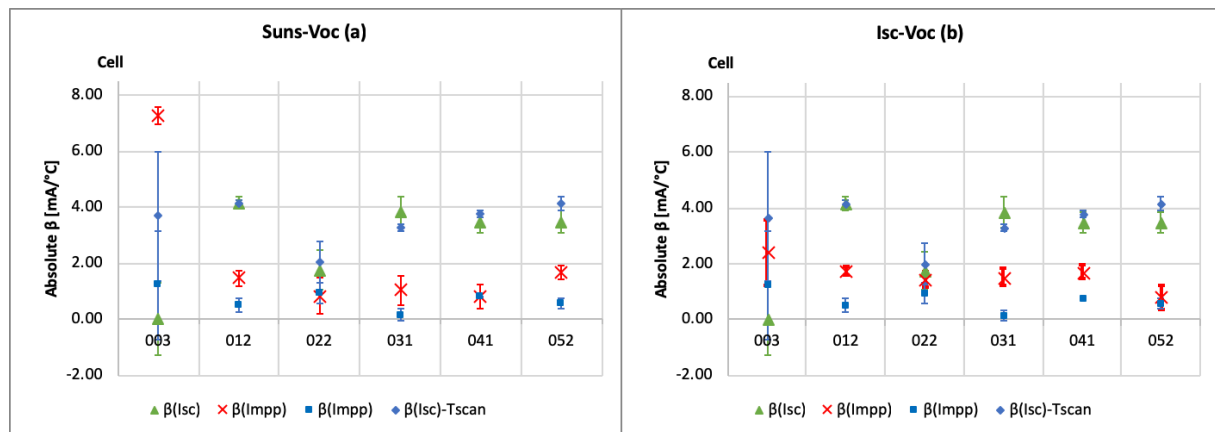
For the Tscan results displayed in both Figure 4-4 (a) and (b), the trend is that  $\beta_{Isc}$  and  $\beta_{Imppp}$  are statistically different. Which here means that all the tested cells, except of cell 022, show higher values for  $\beta_{Isc}$  than for  $\beta_{Imppp}$ , and there is no overlap in the standard deviation. The standard deviation is virtually zero for all the cells Tscan results. Other than the difference in  $\beta_{Isc}$  and  $\beta_{Imppp}$  there are little other trends to be found. The  $\beta_{Imppp}$  of cell 034 is almost zero in the Tscan results, and this is also the cell with the largest difference between  $\beta_{Isc}$  and  $\beta_{Imppp}$ .

For the Suns-Voc results displayed in Figure 4-4 (a), results differ from cell to cell and there is not found any clear systematic trends for  $\beta_{Isc}$  and  $\beta_{Imppp}$ . For all cells except cell 022 and 027, the

difference between  $\beta_{Isc}$  and  $\beta_{Impp}$  is seen as statistically significant, since there is no overlapping of standard deviations and there is a visible gap separating the two.  $\beta_{Isc}$  is generally larger than  $\beta_{Impp}$ , except of cell 012 where the opposite is clear and for the cells with overlapping results it cannot be said as a certain result. The Suns-Voc results are generally in the same size as the Tscan result with slightly larger variation in the different cells.

For the Isc-Voc results displayed in Figure 4-4 (b),  $\beta_{Isc}$  is vertically identical to  $\beta_{Isc}$  from the Suns-Voc measurements,  $\beta_{Impp}$  however is generally lower than for the other measurements. A trend for the Isc-Voc is that  $\beta_{Isc}$  is larger than  $\beta_{Impp}$ , except of cell 012 and 027, where the standard deviation is overlapping between the cells and there is not a clear difference.  $\beta_{Impp}$  values for cell 005, 012 and 034 all have standard deviation reaching in to negative values.

### 4.3.2 PERC 0.5 cells



Figur 4-5 (a) and (b) PERC 0.5  $\beta$  for Isc and Imp

Figure 4-5 is presenting  $\beta_{Isc}$  and  $\beta_{Impp}$  from six PERC 0.5 cells measured using Suns-Voc and Tscan in Figure 4-5(a) and using Isc-Voc and Tscan in Figure 4-5(b).

In Figure 4-4 (a) and (b), all three measuring techniques gives similar results for  $\beta_{Isc}$  and  $\beta_{Impp}$ , except of irregularities in cell 003, therefor the main trends are valid for all three. All the tested cells show higher values for  $\beta_{Isc}$  than for  $\beta_{Impp}$ , except of cell 003 and 022, where the standard deviation is overlapping, all the cells have statistically different  $\beta_{Isc}$  from  $\beta_{Impp}$ . The value of  $\beta_{Isc}$  is similar for all cells except 003, where  $\beta_{Isc}$  is lower for Suns-Voc and Isc-Voc results. Cell 003 have significantly larger standard deviation errors then the rest of the cells in Tscan results and noticeably low  $\beta_{Isc}$  for Suns-Vos and Isc-Voc, this will be commented more in the discussion in the end of the chapter. After cell 003,  $\beta_{Impp}$  is generally larger in the Isc-Voc results than for the other measurements.

### 4.3.3 PERC 1.3 cells

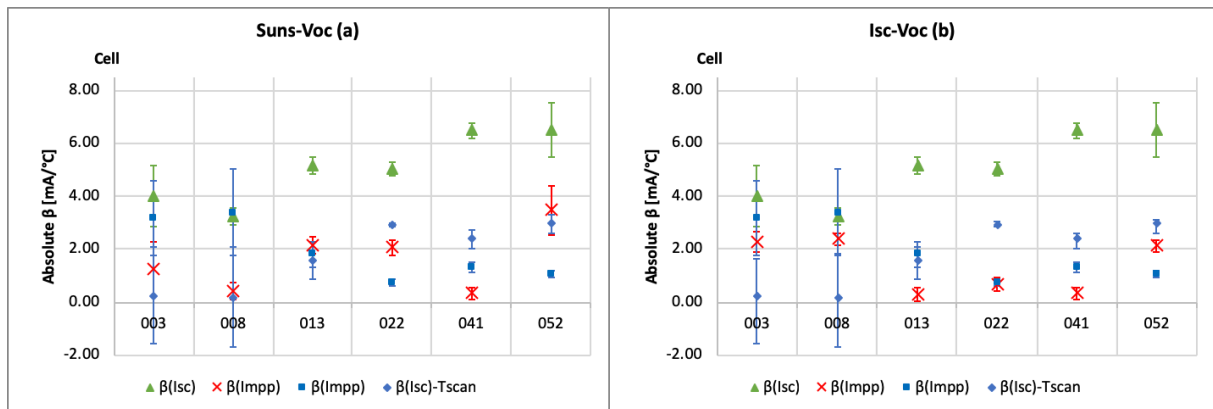


Figure 4-6 (a) and (b) PERC 1.3  $\beta$  for Isc and Impp

Figure 4-6 is presenting  $\beta_{Isc}$  and  $\beta_{Impp}$  from six PERC 1.3 cells measured using Suns-Voc and Tscan in Figure 4-6(a) and using Isc-Voc and Tscan in Figure 4-6(b).

For the Tscan results displayed in both Figure 4-6 (a) and (b),  $\beta_{Isc}$  and  $\beta_{Impp}$  have overlapping standard deviations for the first three cells. For the first two the standard deviation is noticeably larger than for the rest of the cells, for Isc it is crossing over to negative numbers. The three higher numbered cells are showing statistical difference for  $\beta_{Isc}$  and  $\beta_{Impp}$  in the Tscan result. The trend from Tscan is that  $\beta_{Isc}$  is higher than  $\beta_{Impp}$ .

For the Suns-Voc and Isc-Voc results displayed in both Figure 4-6 (a) and (b),  $\beta_{Isc}$  and  $\beta_{Impp}$  is significantly different, with  $\beta_{Isc}$  as the larger value of the two and no overlapping in the standard deviations for any of the cells.  $\beta_{Isc}$  is virtually identical for both Suns-Voc and Isc-Voc results and it is rising in value in the higher cell numbers, whereas  $\beta_{Impp}$  has no noticed trend.

#### 4.4 Discussion for $I_{sc}$ and $I_{mpp}$

The reason for measuring  $I_{sc}$  and  $I_{mpp}$  and calculating  $\beta_{I_{sc}}$  and  $\beta_{I_{mpp}}$  was to do an experimental investigation to see to what degree  $\beta_{I_{sc}}$  is equal to  $\beta_{I_{mpp}}$ . It is also interesting to see if any trends are the same for temperature dependency in voltage and current. The reason for having  $\beta$ -data from Suns-Voc and  $I_{sc}$ -Voc in the same figures was to investigate the other part of the question, "How much is  $R_s$  affecting the difference between  $\beta_{I_{sc}}$  and  $\beta_{I_{mpp}}$ ".

Generally, the results show that  $\beta$  for current is more chaotic than for voltage data. Results compared between the different measuring techniques are showing less visible trends for  $\beta_{I_{sc}}$  and  $\beta_{I_{mpp}}$  than for  $\beta_{V_{oc}}$  and  $\beta_{V_{mpp}}$ . There are less systematic differences between Tscan data and the two other methods. This is probably because  $R_s$  should have little or no effect on the current.

For most of the cells overall the  $\beta_{I_{sc}}$  tends to be larger than  $\beta_{I_{mpp}}$ , however in all three sets of cells there are some cells that either shows the opposite result or in other way are distinguishable from the rest. This variation in result may also be caused by the measuring process, which is harder for current than for voltage. For almost all cells the  $\beta_{I_{sc}}$  results are virtually identical for Suns-Voc and  $I_{sc}$ -Voc, which should be noticed since the current is recorded differently as mentioned in Chapter 2.7. I had expected some more variation in  $\beta_{I_{sc}}$  between Suns-Voc and  $I_{sc}$ -Voc when the parameters are so small.

In the results for both sets of PERC cells the  $\beta_{I_{sc}}$  for Suns-Voc and  $I_{sc}$ -Voc is larger in the higher cell numbers, the  $\beta_{I_{mpp}}$  does not show any significant change. No trends were found between Tscan and the number of the cell. This might be an indication that position in the silicon block plays less of a role for the  $\beta$  of current.

The error bars displaying standard deviation of slope for each  $\beta$  is varying some from cell to cell, however some cells it is more prominent like in cell 003 in the PERC 0.5 results. In Figure 4-5 results for cell 003 differs from the rest, most in Tscan results but also in  $I_{sc}$ -Voc results. After looking at the specific data for cell 003 it is clear that the reason is an unusually high current at 25°C. This is also the case for the case for the  $I_{sc}$ -Voc results, here the current is also unusually high for measurements at 35°C. The high values are consistent for all measurements for each temperature, which indicates that the error is not in measuring. Higher standard deviation indicates less consistency in the data and gives less room for assumptions. The reason for the individual differences is hard to find, since there are many factors that can cause differences in measuring accuracy.

## Chapter 5: Conclusion

Lab work including light soaking, IV measurements using temperature scans, Suns-Voc and Isc-Voc measurements at different temperatures have been carried out to give experimental results for the temperature coefficient of key parameters in a silicon solar cell.

Three types of multicrystalline cells was measured using a NeonSee AAA sun simulator, for a total of 18 tested cells all produced by Elkem Solar. Measurements are done for normal operational temperatures for a solar cell, from 25°C to 65°C. The different cells tested was Al-BSF, PERC 0.5 and PERC 1.3 cells. The measurement data have been calculated using Excel give  $\beta$  results for Voc, Vmpp, Isc and Impp. Then the main question, “to what degree is the temperature coefficient equal for Voc and Vmpp and how does series losses affect the two”, have been investigated. The same question for Isc and Impp have also been investigated. Together these steps are giving the conclusions in the following paragraphs.

Results from the analysed Tscan measurement results is showing a trend where the  $\beta_{Voc}$  is statistically significant different from  $\beta_{Vmpp}$ . This is concluded based on the results where 15 out of the 18 cells tested show  $\beta_{Voc}$  having a larger value than  $\beta_{Vmpp}$ , without any overlapping in the standard deviation. The difference was most significant for the Al-BSF cells, nevertheless it was also strong in the two types of PERC cells. A rise of the value for both  $\beta_{Voc}$  and  $\beta_{Vmpp}$  was also observed from the lower to the higher cell numbers for all three types of cells.

Results from the analysed Suns-Voc and Isc-Voc measurements are showing the same trend of  $\beta_{Voc}$  being statistically significant different to  $\beta_{Vmpp}$  as the Tscan results, however the level of certainty is lower. This lower certainty is based on more variation in the results from the Suns-Voc and Isc-Voc data. For most of the cells calculated standard deviation is very low, which may change if more lab testing is done on the individual cells. However, the standard deviation is smaller for the two sets of PERC cells than for the Al-BSF cells, which is positive since the PERC cells were measured three times per temperature step while the Al-BSF cells were tested once per temperature step. The lower standard deviation of slope for the cells with more measurements builds confidence in the accuracy of the lab work.

As for the effect of  $R_s$ , the difference in results between the Tscan measuring technique and the Suns-Voc and Isc-Voc techniques have been analysed. Tscan is giving the IV data with  $R_s$  while Suns-Voc and Isc-Voc is giving IV data without  $R_s$ . The trend for all three sets of cells is that  $\beta_{Voc}$  have similar values for all three measurement techniques, while  $\beta_{Vmpp}$  is noticeably smaller for the Tscan results. The trend of lower values for  $\beta_{Vmpp}$  from Tscan measurements indicates that  $R_s$  has a negative effect on the  $\beta_{Vmpp}$  and is part of the reason the difference in  $\beta_{Voc}$  and  $\beta_{Vmpp}$ .

Generally, the results show that  $\beta$  for current is more varying than for voltage data. Results compared between the different measuring techniques are showing less visible trends for  $\beta_{Isc}$  and  $\beta_{Impp}$  than for  $\beta_{Voc}$  and  $\beta_{Vmpp}$ . There are less systematic differences between Tscan data and the two other methods. This is probably because  $R_s$  should have little or no effect on the current.

## 5.1 Future Work

This thesis is showing several interesting trends in its conclusion. These trends are indications which may evolve the understanding of the effect different temperatures have on silicon solar cells. A good understanding of temperature in solar cells is necessary to further expand the technology.

The sample size and the limited number of tests done in the work for this thesis does not give enough clear results to be able to state any hard evidence for the questions being asked. There are however trends seen in the results which are good indications for the right answers.

Future work may be to test more types of silicon cells and a wider range of cell numbers. This may contribute to strengthen the trends found in this thesis or to discover other trends. By measuring a wider spread of cell numbers there may also be possible to investigate the effect of cell position in the silicon ingot.

## Chapter 6: List of References

- [1] K. Bithas and P. Kalimeris, "A Brief History of Energy Use in Human Societies," 2016, pp. 5-10.
- [2] K. A. H. Rosvold, Knut, "Solenergi," *Store norske leksikon*, 2017.
- [3] REN21, "Global Status Report 2018," 2018.
- [4] I. E. Agency, "IEA-PVPS Annual Report 2016," *Photovoltaic Power Systems Programme*, 2017.
- [5] P. Edurne Zoco, "IHS Markit Analysts to Discuss Solar Industry Trends at SNEC PV Power Expo 2017 and its First Solar Workshop," I. Markit, Ed., ed, 2017.
- [6] M. A. G. Y. H. E. D. D. H. L. J. H.-E. A. W. Ho-Baillie, "Solar cell efficiency tables (version 51)," in "Progress in photovoltaics research and application. , 2018, Vol.26(1), p.3-12," 2018, Available: <https://onlinelibrary.wiley.com/doi/full/10.1002/pip.2978>.
- [7] D. S. Philipps, "Photovoltaics Report," Fraunhofer ISE and Werner Warmuth, PSE Conferences & Consulting GmbH2018, Available: <https://www.ise.fraunhofer.de/en/publications/studies/photovoltaics-report.html>.
- [8] F. H. Alharbi and S. Kais, "Theoretical limits of photovoltaics efficiency and possible improvements by intuitive approaches learned from photosynthesis and quantum coherence," *Renewable and Sustainable Energy Reviews*, vol. 43, pp. 1073-1089, 2015/03/01/ 2015.
- [9] O. D. R. V. M. A. Green, *THERMAL BEHAVIOR OF PHOTOVOLTAIC DEVICES*. Springer International Publishing, 2017.
- [10] M. A. Green, *SOLAR CELLS*. Prentice Hall: The University of New South Wales, 1998.
- [11] D. L. King, J. A. Kratochvil, and W. E. Boyson, "Temperature coefficients for PV modules and arrays: measurement methods, difficulties, and results," in *Conference Record of the Twenty Sixth IEEE Photovoltaic Specialists Conference - 1997*, 1997, pp. 1183-1186.
- [12] Nick84, "Solar spectrum," ed, 2013.
- [13] M. A. G. Stuart R. Wehham, Muriel E. Watt and Richard Corkish, "Applied photovoltaics ". 2007, p.^pp. Pages.
- [14] Hitachi. *What are semiconductors*. Available: <https://www.hitachi-hightech.com/global/products/device/semiconductor/history.html>
- [15] C. Honsberg and a. S. Bowden. (2018). *PN Junction Introduction* Available: <https://www.pveducation.org/pvcdrom/pn-junctions/introduction-to-semiconductors>
- [16] greenrhinoenergy, "The Photo-effect," ed.
- [17] H. Hidayat, P. I. Widenborg, and A. G. Aberle, "Large-area Suns-Voc Tester for Thin-film Solar Cells on Glass Superstrates," *Energy Procedia*, vol. 15, pp. 258-264, 2012/01/01/ 2012.
- [18] A. Thomason. *How Solar Panels Work*. Available: <https://www.ucsusa.org/clean-energy/renewable-energy/how-solar-panels-work#.W-voOy2ovaY>
- [19] S. magazine, ed.
- [20] C. Honsberg and a. S. Bowden. (2018). *Solar cell operation*. Available: <https://www.pveducation.org/pvcdrom/ideal-solar-cells>
- [21] U. o. Waterloo. *Quartz*. Available: <https://uwaterloo.ca/earth-sciences-museum/resources/detailed-rocks-and-minerals-articles/quartz>
- [22] G. r. energy. (2016). *PV manufacturing*. Available: [http://www.greenrhinoenergy.com/solar/technologies/pv\\_manufacturing.php](http://www.greenrhinoenergy.com/solar/technologies/pv_manufacturing.php)
- [23] G. Fisher, M. Seacrist, and R. W. Standley, *Silicon Crystal Growth and Wafer Technologies*. 2012, pp. 1454-1474.
- [24] T. F. Ciszek, G. H. Schwuttke, and K.-H. Yang, *Solar-Grade Silicon by Directional Solidification in Carbon Crucibles*. 1979, pp. 270-277.



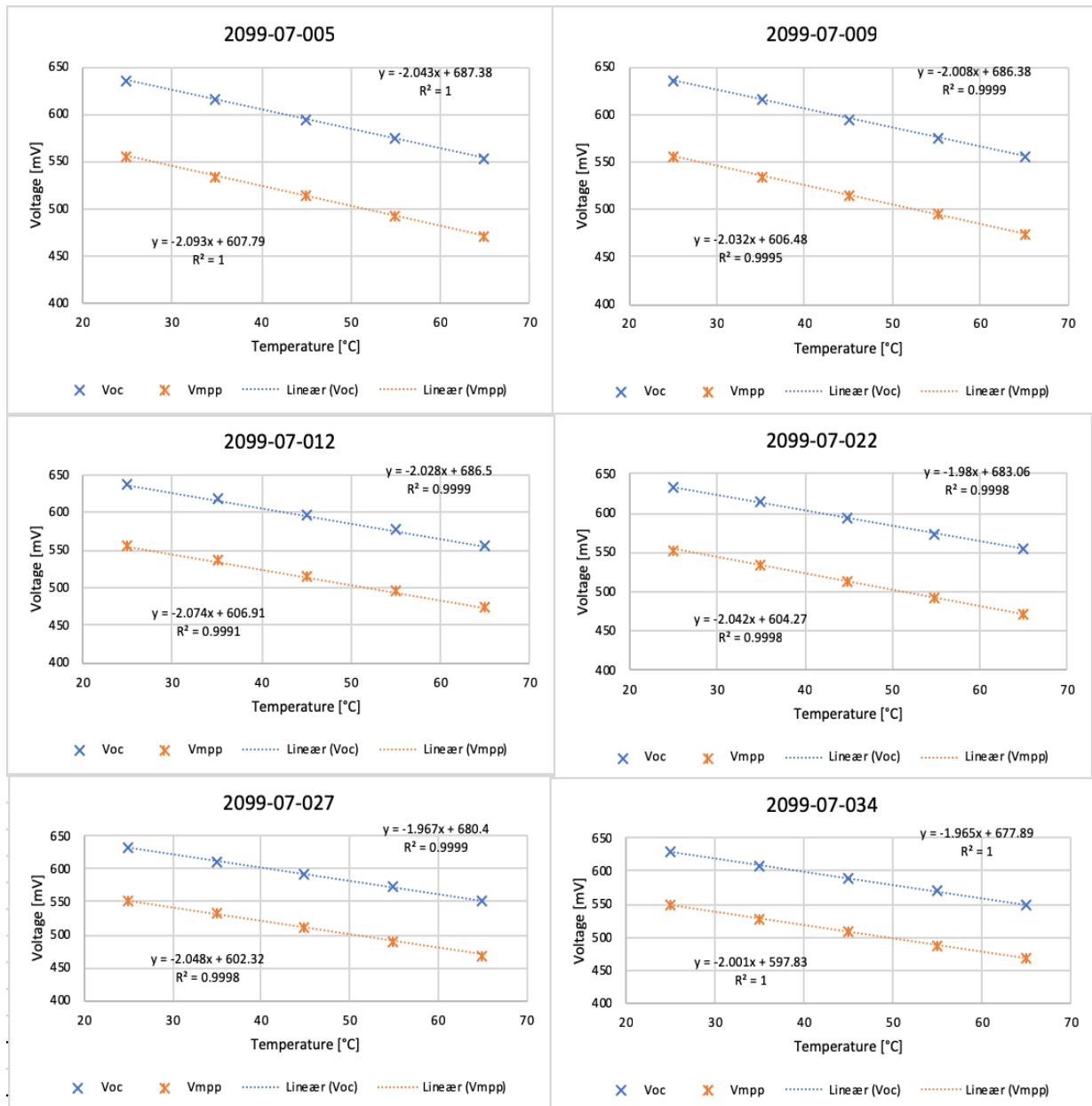
- [25] K. Krauß, F. Fertig, D. Menzel, and S. Rein, *Light-induced Degradation of Silicon Solar Cells with Aluminiumoxide Passivated Rear Side*. 2015, pp. 599-606.
- [26] V. Unsur, B. Hussain, and A. Ebong, *Complete recovery of light induced degradation of Cz silicon solar cells with rapid thermal processing*. 2016, pp. 0717-0719.
- [27] NeonSee, "Sun Simulator," ed, 2016.
- [28] S. M. Ross, "CHAPTER 12 - Linear Regression," in *Introductory Statistics (Third Edition)*, S. M. Ross, Ed. Boston: Academic Press, 2010, pp. 537-604.
- [29] F. A. Morrison, "Obtaining Uncertainty Measures on Slope and Intercept of a Least Squares Fit with Excel's LINEST," M. T. University, Ed., ed, 2014.

## Chapter 7: Appendix

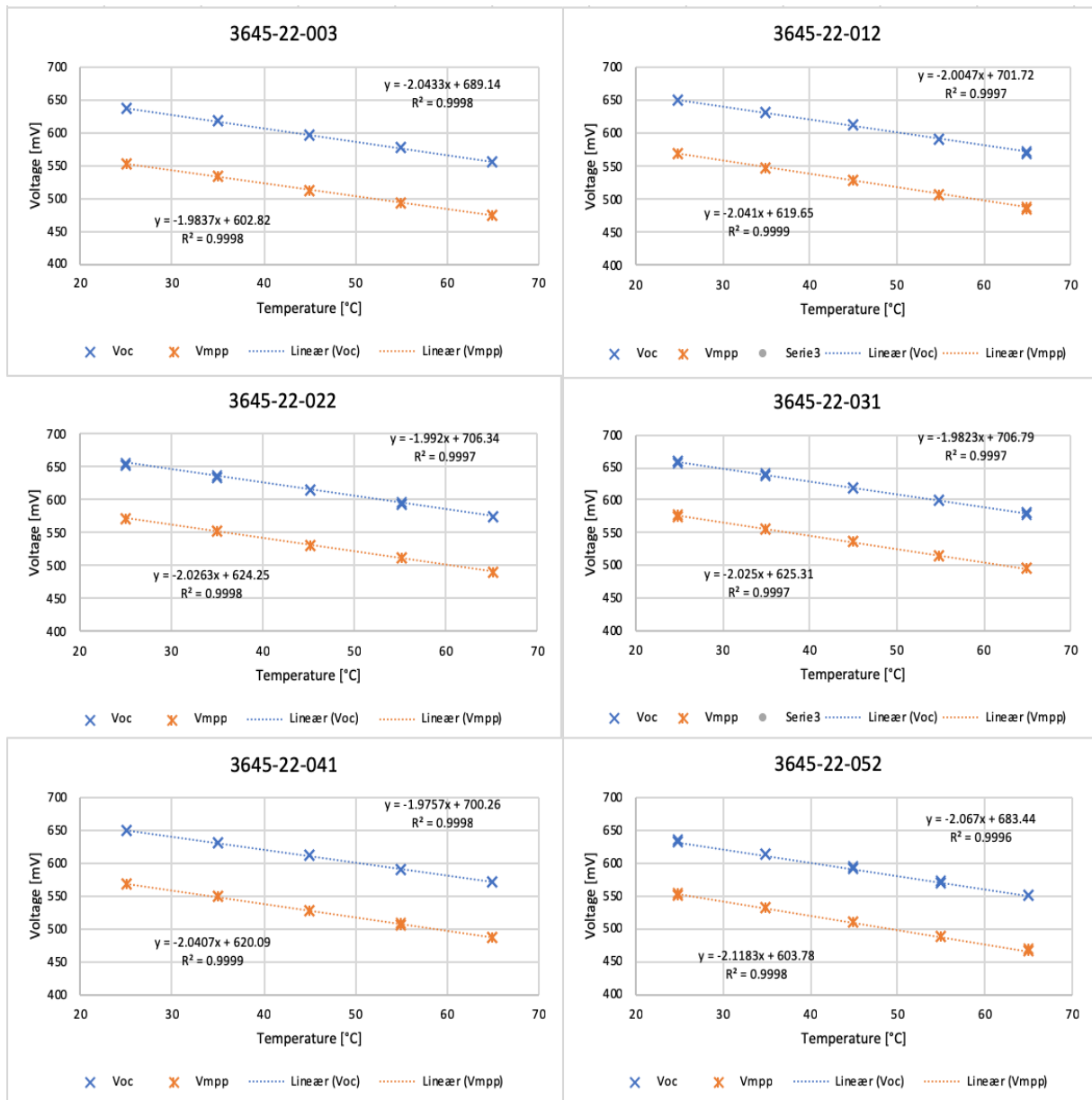
### 7.1 Appendix A

Voc and Vmpp here is from Suns-Voc measurements.

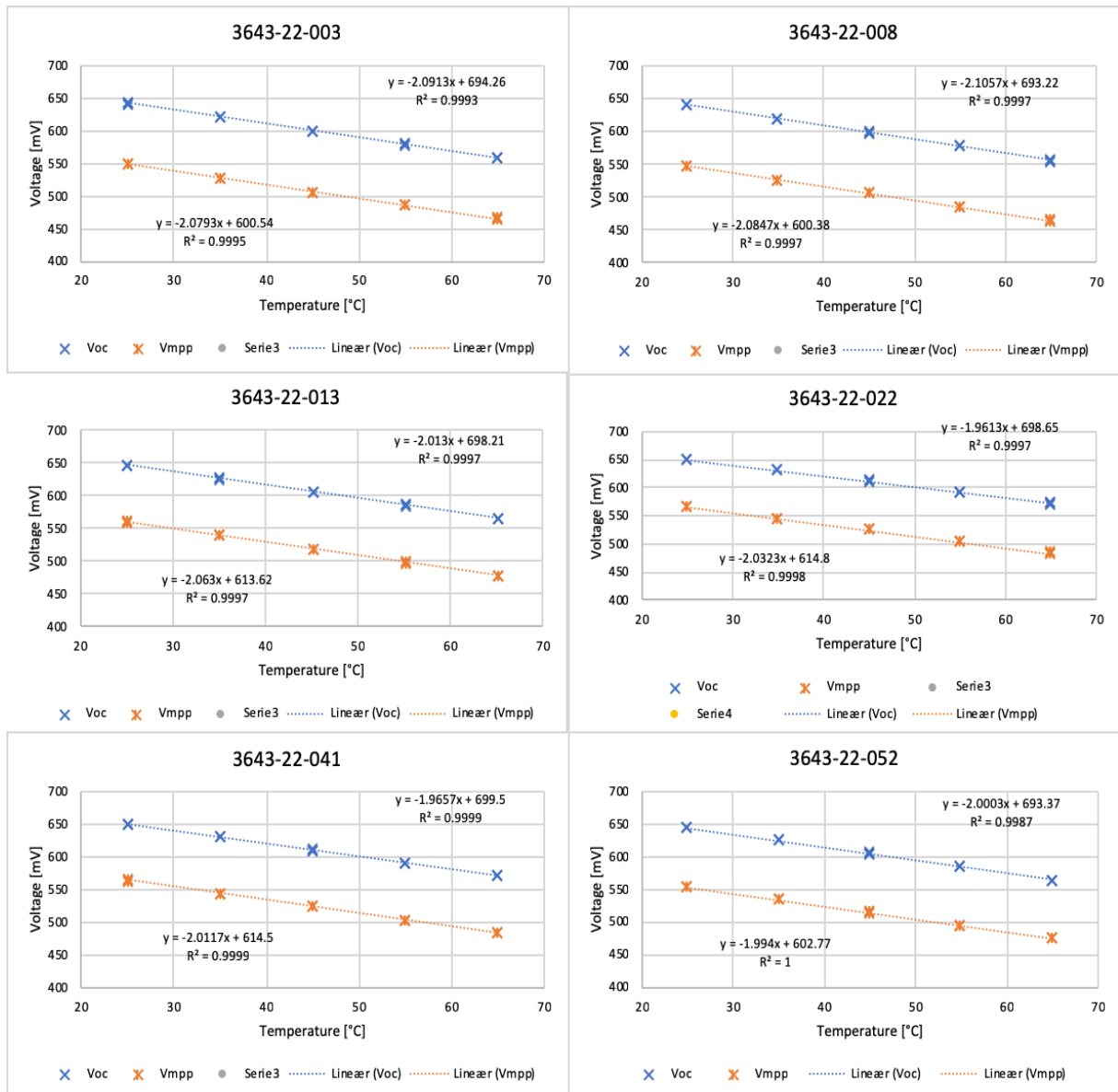
Voc and Vmpp per temperature for Al-BSF cells



## Voc and Vmpp per temperature for PERC 0.5 cells



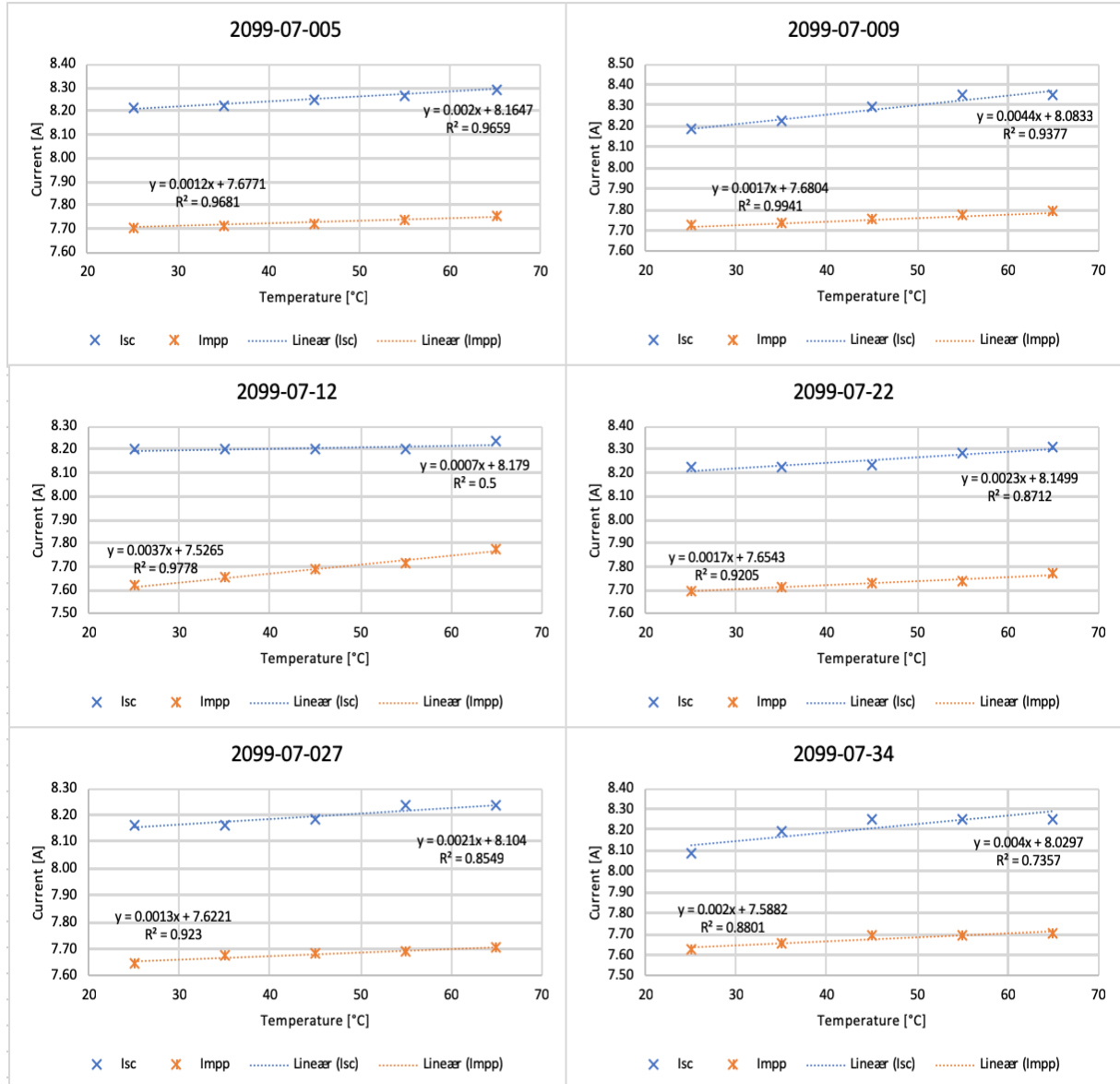
### Voc and Vmpp per temperature for PERC 1.3 cells



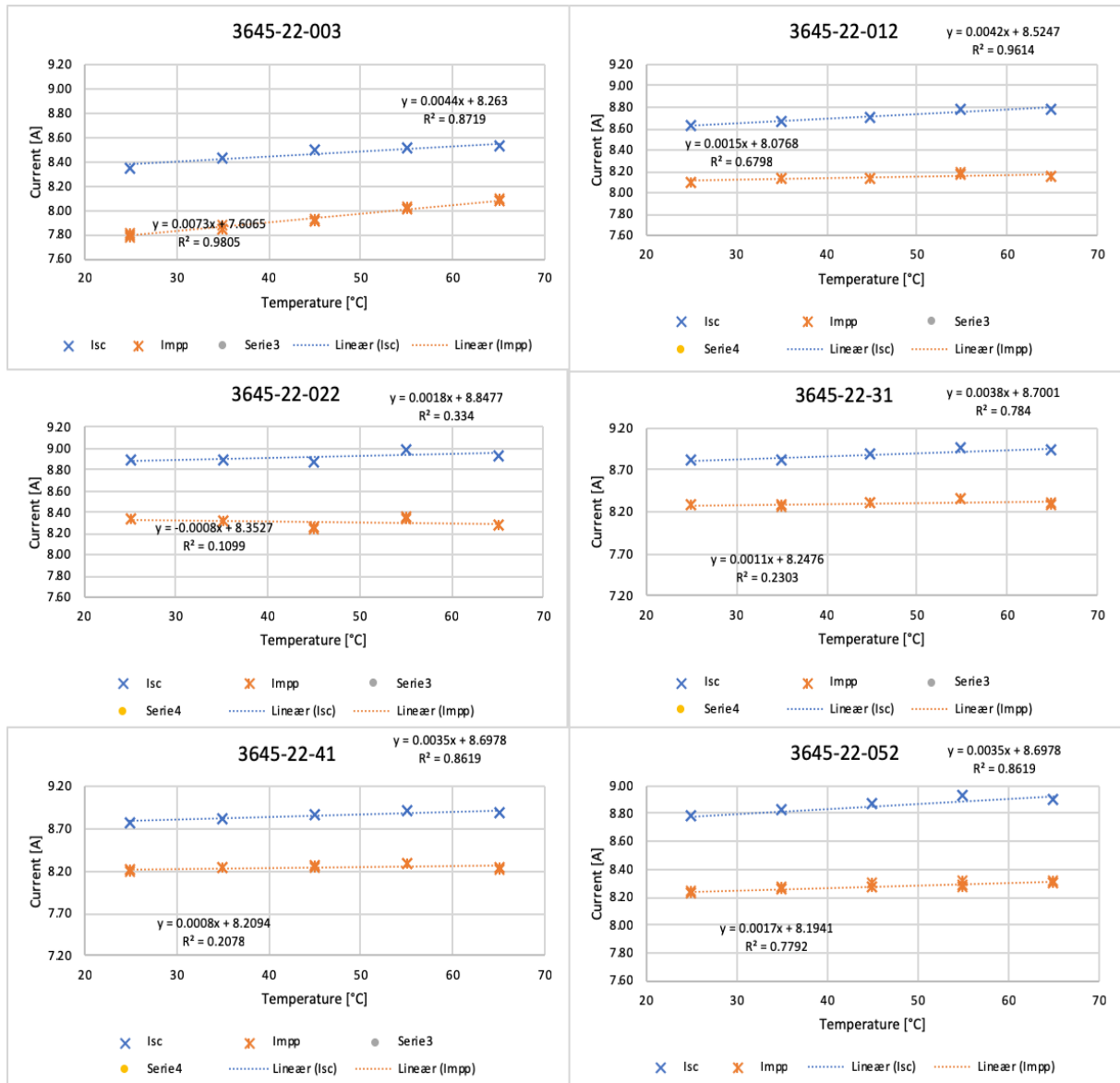
## 7.2 Appendix B

Isc and Impp here is from Suns-Voc measurements.

Isc and Impp per temperature for Al-BSF



### Isc and Imp per temperature for PERC 0.5 cells



### Isc and Impp per temperature for PERC 1.3 cells

